Temperature jump and Knudsen layer in rarefied molecular gas

Physics of Fluids
AIP Publishing

Temperature jump and Knudsen layer in rarefied molecular gas

Wei Su (苏微),[1] Qi Li (李琪),[2] Yonghao Zhang (张勇豪),[1] and Lei Wu (吴雷)[2]
[1)] *School of Engineering, The University of Edinburgh, Edinburgh EH9 3FB, United Kingdom*
[2)] *Department of Mechanics & Aerospace Engineering, Southern University of Science and Technology, Shenzhen 518055, P.R. China*

(*Electronic mail: wul@sustech.edu.cn)

(Dated: 15 February 2022)

The temperature jump problem in rarefied molecular (diatomic and polyatomic) gases is investigated based on a one-dimensional heat conduction problem. The gas dynamics is described by a kinetic model, which is capable to recover the general temperature and thermal relaxation processes predicted by the Wang-Chang Uhlenbeck equation. Analytical formulations for the temperature jump coefficient subject to the classical Maxwell's gas-surface interaction are derived via the Chapman-Enskog expansion. Numerically, the temperature jump coefficient and the Knudsen layer function are calculated by matching the kinetic solution to the Navier-Stokes prediction in the Knudsen layer. Results show that the temperature jump highly depends on the thermal relaxation processes: the values of the temperature jump coefficient and the Knudsen layer function are determined by the relative quantity of the translational thermal conductivity to the internal thermal conductivity; a minimum temperature jump coefficient emerges when the translational Eucken factor is $4/3$ times of the internal one. Due to the exclusion of the Knudsen layer effect, the analytical estimation of the temperature jump coefficient may possess large errors. A new formulation, which is a function of the internal degree of freedom, the Eucken factors, and the accommodation coefficient, is proposed based on the numerical results.

I. INTRODUCTION

A gas flow may be modeled either by the Navier-Stokes equations as a continuum or by the kinetic equation as a myriad of discrete molecules. The continuous description equipped with non-slip velocity and non-jump temperature conditions at the solid boundary is only valid when the mean free path of gas molecules λ is significantly smaller than the characteristic flow length L; otherwise, the kinetic description at the mesoscopic level of molecular velocity distribution function should be adopted. Compared to the continuum equations, a numerical solving of the kinetic equation is much more expensive, since the independent variables are increased with the number of physical variables (e.g., position, velocity, and internal energy) on which the state of every gas molecule depends. Therefore, for flows having moderate Knudsen number ($Kn = \lambda/L$) where the kinetic effect resulted from the inhomogeneity introduced by the solid boundary is only important within the Knudsen layer of thickness $O(\lambda)$, it is very attractive to effectively quantify the flow behaviors though the continuum equations incorporated velocity slip and temperature jump boundary conditions; while the actual kinetic effect can be taken into account by the Knudsen layer function.

The temperature jump at the interface between a solid wall and an adjacent gas is traditionally defined as the difference between the temperature of the wall and the temperature arising at the wall from a linear extrapolation of the temperature curve of gas beyond the Knudsen layer[1,2], written as

$$T_e = T_w + \zeta_T \frac{\mu}{p}\sqrt{\frac{2k_B T_w}{m}}\frac{\partial T}{\partial n}, \quad \text{at wall}, \qquad (1)$$

where T_e and T_w are the linearly extrapolated gas temperature and the wall temperature, respectively; ζ_T is the constant temperature jump coefficient (TJC); μ is the shear viscosity of gas; p is the local gas pressure; k_B is the Boltzmann constant;

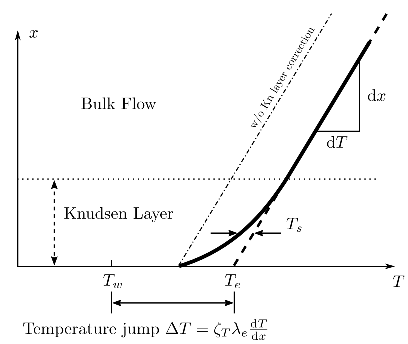

FIG. 1. The temperature jump is defined as the difference between the wall temperature T_w and the temperature at the wall T_e from a linear extrapolation of the temperature curve in the bulk region; ζ_T is the temperature jump coefficient, and λ_e is the equivalent mean free path of gas molecules; The Knudsen layer function T_s describes the deviation of the linearly extrapolated temperature (dash line) from the true temperature (solid line) in Knudsen layer.

m is the mass of gas molecules; and $\partial/\partial n = \boldsymbol{n}\cdot\nabla$ with $\boldsymbol{n}$ being the unit outward normal vector at the wall, respectively. The Knudsen layer function is defined as the deviation of the linearly extrapolated temperature from the true temperature in the Knudsen layer. Figure 1) shows a schematic diagram of the problem. A rough estimation of the coefficient ζ_T is given by[3]

$$\zeta_T = \frac{\gamma\sqrt{\pi}}{(\gamma+1)\,Pr}\frac{2-\alpha_0}{\alpha_0}, \qquad (2)$$

where γ is the specific heat ratio; Pr is the Prandtl number; and α_0 is the constant accommodation coefficient in the classical Maxwell's boundary condition, representing the fraction of incident molecules that are diffusely reflected at the wall. This estimation is obtained on the assumption that the velocity distribution function of gas molecules does not vary within the Knudsen layer. Note that velocity gradients near the wall may lead to temperature jump as well, however this effect is usually ignored since it is small and cannot be controlled in experiments[4].

More rigorous analysis can be done by matching the kinetic solution inside the Knudsen layer to the outer Navier-Stokes solution. Taking advantages of the improvement in solving kinetic equations, TJCs have been obtained based on the Bhatnagar-Gross-Krook (BGK) kinetic model[5,6], Shakhov model[7], and the linearized Boltzmann equation[8–12]. It is shown that under the fully diffuse reflection at walls, the TJC varies in a small range from model to model; the one obtained from the Shakhov model equation is very close to those obtained from the Boltzmann equation with more realistic Lennard-Jones potentials. In practice, a value of $\zeta_T = 1.95$ is recommended[2]. The dependence of the jump coefficient on the accommodation coefficient was approximated as

$$\zeta_T = \frac{15\sqrt{\pi}}{16}\left(\frac{2-\alpha_0}{\alpha_0}+0.173\right) \tag{3}$$

by Welander[2] or as

$$\zeta_T = \frac{15\sqrt{\pi}}{16}\frac{2-\alpha_0}{\alpha_0}\left(1+0.1621\alpha_0\right) \tag{4}$$

by Loyalka [13]. Both the estimations are based on the solutions of the BGK equation. The TJCs subjected to the Cercignani-Lampis gas-surface interaction[7,12], as well as those of gas mixtures[14,15] have also been calculated. A comprehensive review and comparison of these data have been reported by Sharipov[2]. Note that the expression (1) is generally a first-order result, which is adequate when $Kn < 0.1$[16]. The second-order temperature jump condition can be derived through the asymptotic expansion of the molecular velocity distribution function[17]; a second jump coefficient emerges along with the second-order derivative of gas temperature at the wall. For steady flows without external heating source, the second jump coefficient is only known, equal to zero, for the BGK model. The second jump coefficients for a problem governed by the Poisson equation, i.e., the steady conduction subject to forcing heating and an unsteady problem subject to time-dependent wall temperature have been obtained[16,18].

Although one more often deals with molecular (diatomic or polyatomic) gases in practical applications, the above mentioned works only considered monatomic gases. When the Boltzmann equation is extended to the Wang-Chang Uhlenbeck (WCU) equation[19] for molecular gases, additional degrees of freedom due to the excitation of internal energies associated with rotations, vibrations, and electrons yield a much more complicated governing system; the internal motions are treated quantum-mechanically and each energy level is assigned with an individual distribution function, making analytical and numerical solutions extremely difficult and expensive. Hitherto the TJC in molecular gases, although very few, are calculated based on kinetic model equations. The probably first estimation was made by Lin[1] from the Morse model for gases with only rotations excited, which is read as

$$\zeta_T = \frac{\gamma\sqrt{\pi}}{(\gamma+1)\,Pr}\left(\frac{2-\alpha_0}{\alpha_0}+0.17\right), \tag{5}$$

implying that ζ_T roughly depends on, considering the gas physical properties, the ratio of the shear viscosity to the thermal conductivity, i.e., the Prandtl number Pr, and the number of internal degrees of freedom that determines the specific heat ratio γ. In the particular case of a monatomic gas when $\gamma = 5/3$ and $Pr = 2/3$, the estimation (5) is reduced to (3). A more comprehensive analysis on both the velocity slip and temperature jump in molecular gases was recently conducted[20]. The slip/jump coefficients and the Knudsen layer functions were obtained through the Chapman-Enskog expansion to the ellipsoidal BGK (ES-BGK) model equation[21,22]. The ES-BGK model contains three adjustable parameters, allowing fitting the experimental values of the shear viscosity, the thermal conductivity, and the bulk viscosity that appears due to the finite time required for the system to distribute energy among the internal degrees of freedom. The results for some typical molecular gases show that the TJC also varies with the bulk viscosity, although not significantly.

In molecular gases, unique transport phenomena, which play important roles in rarefied molecular gas dynamics[23], take place because of the exchange of translational and internal energies. It can be shown[24,25] that the relaxation rate of between the translational and internal energies determines the ratio of the bulk viscosity to the shear viscosity, and the thermal relaxation rates of translational and internal heat fluxes determine the thermal conductivities, comprising of translational and internal parts. Note that the thermal conductivity (or Pr) in expression (5) is an overall measurement combining both the translational and internal contributions. Few data on the temperature jump coefficient in molecular gases has been reported. To the authors' awareness, comprehensive study on the effects of the unique relaxation processes in molecular gases, especially the thermal relaxations, has been far overlooked. However, we will discover later that the TJC and Knudsen layer function have strong dependence on the relaxation rates of heat fluxes, even though the total thermal conductivity is fixed.

This work aims to fill the above knowledge gap. Credibility of the analysis is highly affected by the accuracy of the kinetic equation and the analytical method or numerical scheme we use. In this paper, the behavior of molecular gas flows is described by a kinetic model introduced by Li *et al.* [25]. Been calibrated and verified through the direct simulation Monte Carlo (DSMC) method, the model has the ability to recover the general temperature and thermal relaxations derived from the Wang-Chang Uhlenbeck equation, and to freely adjust the relaxation rates, the influence of which thus can be investigated. This cannot be attained by any other kinetic models[26–29]. The remainder of the paper is arranged as follows. The kinetic description for the dynamics of rarefied molecular gases including the kinetic equation and gas-surface interaction model is given in §II. A rough estimation of the TJC subject to the Maxwell's boundary condition, is derived by assuming a first-order Chapman-Enskog velocity-energy distribution function. The details are also given in §III. The one-dimensional steady heat conduction problem and the assumptions to numerically calculate the TJC and the Knudsen layer function are presented in §IV, where the numerical scheme is briefly described. The results and discussions are demonstrated in §V, followed by an empirical but more accurate formulation for the TJC. Some conclusions are presented in §VI. The paper is one of our serial works on the slip/jump coefficients, where the thermal velocity slip in molecular gases were studied in Ref.[30].

II. GOVERNING EQUATIONS

The gaseous kinetic description for rarefied molecular gases is presented in this section. We consider flow under the constraint that a gas molecule has three translational and d rotational degrees of freedom. The rotational energy can be expressed by a single continuous variable I as the way of classical mechanics.

A. Gas kinetic equation

Solving WCU equation for molecular gases is unrealistic due to its high complexity and excessive computational burden. Therefore, kinetic models are proposed to imitate the behaviour of the WCU equation. The typical ones are extended from BGK-type model equations of monatomic gas, such as Rykov model[29], ellipsoidal-statistical BGK model[21,31], Wang model[32]. Recently, Wu model[25,33] is proposed to improve the accuracy of model equations by using Boltzmann collision operator of monatomic gases for elastic collisions, and incorporating the thermal relaxation rates to recover the correct transport coefficients. Thus, Wu model is adopted in the present work and briefly introduced as following.

In spatial-homogeneous systems, on an average sense, the relaxation of the temperature associated with the rotational energy, denoting as T_r is described by the Jeans–Landau equation

$$\frac{\partial T_r}{\partial \hat{t}} = \frac{p_t}{\mu}\frac{T-T_r}{Z}, \tag{6}$$

where $\hat{t}$ is the time, p_t is the kinetic pressure; μ is the gas shear viscosity, Z is the rotational collision number (roughly speaking, a gas molecule would experience one inelastic collision in every Z binary collisions), and T is the overall temperature calculated from the weighted sum of the translational temperature T_t and the rotational temperature T_r as $T=(3T_t+dT_r)/(3+d)$. The relaxations of the translational heat flux $\boldsymbol{Q}_t$ and the rotational heat flux $\boldsymbol{Q}_r$ generated from the transfer of energies satisfy the following general relations[34,35]

$$\begin{bmatrix} \partial \boldsymbol{Q}_t/\partial \hat{t} \\ \partial \boldsymbol{Q}_r/\partial \hat{t} \end{bmatrix} = -\frac{p_t}{\mu}\begin{bmatrix} A_{tt} & A_{tr} \\ A_{rt} & A_{rr} \end{bmatrix}\begin{bmatrix} \boldsymbol{Q}_t \\ \boldsymbol{Q}_r \end{bmatrix}, \tag{7}$$

where $\boldsymbol{A}=[A_{ij}]$ ($i,j=t$ or r) is the matrix of relaxation rates possessing positive eigenvalues. These unique transport processes (6) and (7) induce the bulk viscosity μ_b, and make the thermal conductivity κ consisting of both the translational and rotational contributions, termed κ_t and κ_r, respectively, thus $\kappa=\kappa_t+\kappa_r$. These transport coefficients are determined as[25]

$$\frac{\mu_b}{\mu} = \frac{2dZ}{3(d+3)}, \tag{8}$$

and

$$\begin{bmatrix} \kappa_t \\ \kappa_r \end{bmatrix} = \frac{k_B\mu}{2m}\begin{bmatrix} A_{tt} & A_{tr} \\ A_{rt} & A_{rr} \end{bmatrix}^{-1}\begin{bmatrix} 5 \\ d \end{bmatrix}. \tag{9}$$

It will be convenient to express the thermal conductivities in terms of the dimensionless factors[36,37]

$$\frac{\kappa m}{\mu k_B} = \frac{3}{2}f_t + \frac{d}{2}f_r = \frac{3+d}{2}f_{eu}, \tag{10}$$

where f_{eu} is the total Eucken factor; f_t and f_r are the translational and rotational Eucken factor, respectively, defined as

$$f_t = \frac{2}{3}\frac{\kappa_t m}{\mu k_B}, \quad f_r = \frac{2}{d}\frac{\kappa_r m}{\mu k_B}, \tag{11}$$

respectively. The values of the Eucken factors can be extracted from experiments[24]. For monatomic gases, $A_{tt}=2/3$ and $A_{tr}=A_{rt}=A_{rr}=0$, so that $f_{eu}=f_t=2.5$ and $f_r=0$.

In practice, gas kinetic models are introduced to reduce the computational complexity arisen in the Wang-Chang Uhlenbeck equation. To guarantee accuracy, it is required that the model equation is capable to interpret the relaxation processes and recover the transport coefficients. To this end, we adopt the following kinetic model, where the state of gas is described by the one-particle velocity-energy distribution function $f(\hat{t},\boldsymbol{X},\boldsymbol{V},I)$ with $\boldsymbol{X}=(X_1,X_2,X_3)$, $\boldsymbol{V}=(V_1,V_2,V_3)$ and $I\geq 0$ being the location, translational velocity and rotational energy of gas molecules, respectively. Macroscopic quantities, such as the number density $n(\hat{t},\boldsymbol{X})$, the bulk velocity $\boldsymbol{U}(\hat{t},\boldsymbol{X})$, the temperatures $T_{t/r}(\hat{t},\boldsymbol{X})$ and heat fluxes $\boldsymbol{Q}_{t/r}(\hat{t},\boldsymbol{X})$ are defined as

$$\left[n, n\boldsymbol{U}, \frac{3}{2}nk_BT_t, \frac{d}{2}nk_BT_r, \boldsymbol{Q}_t, \boldsymbol{Q}_r\right] = \iint \left[1, \boldsymbol{V}, \frac{mC^2}{2}, I, \boldsymbol{C}\frac{mC^2}{2}, \boldsymbol{C}I\right] f \mathrm{d}\boldsymbol{V}\mathrm{d}I, \tag{12}$$

where $\boldsymbol{C}=\boldsymbol{V}-\boldsymbol{U}$ is the peculiar velocity. We also defined the pressures as $p_t=nk_BT_t$, $p_r=nk_BT_r$ and $p=nk_BT$ in terms of the translational, rotational, and overall temperatures, respectively.

In the absence of external force, the evolution of f is governed by

$$\frac{\partial f}{\partial \hat{t}} + \boldsymbol{V}\cdot\frac{\partial f}{\partial \boldsymbol{X}} = \underbrace{\frac{g_t - f}{\hat{\tau}}}_{elastic} + \underbrace{\frac{g_r - g_t}{Z\hat{\tau}}}_{inelastic}, \tag{13}$$

where $\hat{\tau} = \mu/p_t$ is the relaxation time related to translational motions, and the terms on the right-hand side of the equation describe the change of f due to elastic and inelastic collisions, respectively. The reference velocity distribution functions g_t and g_r, expanding about the equilibrium $f_0 = E_t(T) \cdot E_r(T)$ in a series of orthogonal polynomials, have the following forms

$$g_t = E_t(T_t) E_r(T_r) \left[1 + \frac{2m\boldsymbol{Q}_t \cdot \boldsymbol{C}}{15 k_B T_t p_t} \left(\frac{mC^2}{2k_B T_t} - \frac{5}{2}\right) + \frac{2m\boldsymbol{Q}_r \cdot \boldsymbol{C}}{d k_B T_t p_r} \left(\frac{I}{k_B T_r} - \frac{d}{2}\right)\right], \tag{14a}$$

$$g_r = E_t(T) E_r(T) \left[1 + \frac{2m\boldsymbol{Q}' \cdot \boldsymbol{C}}{15 k_B T p} \left(\frac{mC^2}{2k_B T} - \frac{5}{2}\right) + \frac{2m\boldsymbol{Q}'' \cdot \boldsymbol{C}}{d k_B T p} \left(\frac{I}{k_B T} - \frac{d}{2}\right)\right], \tag{14b}$$

where

$$\begin{aligned} E_t(T) &= n \left(\frac{m}{2\pi k_B T}\right)^{3/2} \exp\left(-\frac{mC^2}{2k_B T}\right), \\ E_r(T) &= \frac{I^{d/2-1}}{\Gamma(d/2)(k_B T)^{d/2}} \exp\left(-\frac{I}{k_B T}\right), \end{aligned} \tag{15}$$

and $\Gamma(\cdot)$ is the gamma function. $\boldsymbol{Q}'$ and $\boldsymbol{Q}''$ are linear combinations of the translational and rotational heat fluxes, which are formulated to recover the relaxations (7), read as

$$\begin{bmatrix} \boldsymbol{Q}' \\ \boldsymbol{Q}'' \end{bmatrix} = \begin{bmatrix} (2-3A_{tt})Z+1 & -3A_{tr}Z \\ -A_{rt}Z & Z(1-A_{rr}) \end{bmatrix} \begin{bmatrix} \boldsymbol{Q}_t \\ \boldsymbol{Q}_r \end{bmatrix}. \tag{16}$$

It is worth noting that this kinetic model can be regarded as a general version of the Rykov kinetic model[29], regarding that the relaxation of heat fluxes in the Rykov model is a special circumstance with $A_{tr} = 0$ and $A_{rt} = 0$. In the limit without translational-rotational energy exchange ($Z \to \infty$, $d = 0$, $A_{tt} = 2/3$ and $A_{tr} = A_{rt} = A_{rr} = 0$), the kinetic model (13) reduces to the Shakhov model equation for monatomic gases[38].

B. Gas-surface interaction model

Considering the gas-wall interaction from the viewpoint of a non-absorbing wall at rest, all the gas molecules hitting the wall with a velocity $\boldsymbol{V}'$ will return to the flows with a new velocity $\boldsymbol{V}$. The velocity-energy distribution function of the molecules in the nearest vicinity of the wall is denoted as

$$f_w = \begin{cases} f^-, & \boldsymbol{V} \cdot \boldsymbol{n} \le 0 \\ f^+, & \boldsymbol{V} \cdot \boldsymbol{n} > 0 \end{cases}, \tag{17}$$

where f^- and f^+ are the distributions of incident and reflected molecules, respectively. The correlation between the incident and reflected distribution functions is determined by the reflection kernel $\mathscr{R}(\boldsymbol{V}' \to \boldsymbol{V})$ as

$$f^+ = \frac{1}{|\boldsymbol{V} \cdot \boldsymbol{n}|} \int_{\boldsymbol{V}' \cdot \boldsymbol{n} < 0} f^-(\boldsymbol{V}') \mathscr{R}(\boldsymbol{V}' \to \boldsymbol{V}) \, \mathrm{d}\boldsymbol{V}'. \tag{18}$$

Under the classical Maxwell's gas-wall interaction model, the distribution function of the reflected molecules is a linear combinations of two extreme situations: specular reflection and fully-diffuse reflection. In the former situation, the wall is assumed perfectly smooth and rigid; when an incident molecule interacts with the wall, its normal velocity is inverse, while the tangential velocity remains unchanged. Thus the reflection kernel is expressed as

$$\mathscr{R}_{spec}(\boldsymbol{V}' \to \boldsymbol{V}) = \delta(\boldsymbol{V}' - \boldsymbol{V} + 2(\boldsymbol{V} \cdot \boldsymbol{n})\boldsymbol{n}), \tag{19}$$

where $\delta(\cdot)$ is the delta function. On the other hand, when an incident molecule interacts with a rough wall with vibrating atoms, energy-exchange occurs between the gas molecule and the solid atoms; the reflected molecules tend to get equilibrium at the wall temperature T_w, and the reflection kernel is given as

$$\mathscr{R}_{diff}(\boldsymbol{V}' \to \boldsymbol{V}) = |\boldsymbol{V} \cdot \boldsymbol{n}| f_0(T_w), \tag{20}$$

where $f_0 = E_t \cdot E_r$ is the equilibrium distribution. With a constant accommodation coefficient α_0, the reflection kernel of the Maxwell's boundary condition is read as

$$\begin{aligned} \mathscr{R}_M(\boldsymbol{V}' \to \boldsymbol{V}) =& \alpha_0 \mathscr{R}_{diff}(\boldsymbol{V}' \to \boldsymbol{V}) \\ &+ (1-\alpha_0)\mathscr{R}_{spec}(\boldsymbol{V}' \to \boldsymbol{V}). \end{aligned} \tag{21}$$

For molecular gases, the reflection kernel can be generalized as

$$f^+ = \frac{1}{|\boldsymbol{V} \cdot \boldsymbol{n}|} \iint_{\boldsymbol{V}' \cdot \boldsymbol{n} < 0} f^-(\boldsymbol{V}', I') \mathscr{R}(\boldsymbol{V}' \to \boldsymbol{V}, I' \to I) \, \mathrm{d}\boldsymbol{V}' \mathrm{d}I', \tag{22}$$

with

$$\begin{aligned} &\mathscr{R}(\boldsymbol{V}' \to \boldsymbol{V}, I' \to I) = \\ &\alpha_0 \frac{|\boldsymbol{V} \cdot \boldsymbol{n}| m^2 I^{d/2-1}}{2\pi \Gamma(d/2)(k_B T_w)^{2+d/2}} \times \exp\left(-\frac{mV^2}{2k_B T_w} - \frac{I}{k_B T_w}\right) \\ &+ (1-\alpha_0)\delta(\boldsymbol{V}' - \boldsymbol{V} + 2(\boldsymbol{V} \cdot \boldsymbol{n})\boldsymbol{n})\,\delta(I - I'), \end{aligned} \tag{23}$$

where I' and I denote the rotational energies of the incident and reflected molecules, respectively.

III. ANALYTICAL ESTIMATION OF TJC

Now we present an analytical estimation of the TJC, which is sought at $Kn \ll 1$. When the system is close to equilibrium, the distribution function can be expanded as $f = f_0 + f_1$ with f_1 the perturbed part to the first order of Chapman-Enskog expansion[39]. By linearizing the reference distribution g_t and g_r at the equilibrium temperature T and considering a static gas system with respect to the wall, it is obtained

$$\begin{aligned} f_1 = f_0 \Bigg\{ & -\frac{\mu}{p}\boldsymbol{C}\cdot\nabla\ln T\left[\left(\frac{mC^2}{2k_BT}-\frac{5}{2}\right)+\left(\frac{I}{k_BT}-\frac{d}{2}\right)\right] \\ & +\frac{T_t-T}{T}\left(1-\frac{1}{Z}\right)\left[\left(\frac{mC^2}{2k_BT}-\frac{3}{2}\right)-\frac{3}{d}\left(\frac{I}{k_BT}-\frac{d}{2}\right)\right] \\ & +\left(1-\frac{1}{Z}\right)\left[\frac{2m\boldsymbol{Q}_t\cdot\boldsymbol{C}}{15k_BTp}\left(\frac{mC^2}{2k_BT}-\frac{5}{2}\right)\right. \\ & \left.+\frac{2m\boldsymbol{Q}_r\cdot\boldsymbol{C}}{dk_BTp}\left(\frac{I}{k_BT}-\frac{d}{2}\right)\right] \\ & +\frac{1}{Z}\left[\frac{2m\boldsymbol{Q}'\cdot\boldsymbol{C}}{15k_BTp}\left(\frac{mC^2}{2k_BT}-\frac{5}{2}\right)\right. \\ & \left.+\frac{2m\boldsymbol{Q}''\cdot\boldsymbol{C}}{dk_BTp}\left(\frac{I}{k_BT}-\frac{d}{2}\right)\right]\Bigg\}. \end{aligned} \tag{24}$$

Following the method introduced by Struchtrup[4], the temperature jump condition is derived by matching the energy fluxes along the normal direction of solids to the ones computed from the distribution function f_w, i.e.,

$$\begin{aligned} \boldsymbol{Q}_t\cdot\boldsymbol{n} &= \int \frac{mC^2}{2}\boldsymbol{C}\cdot\boldsymbol{n}f_w\mathrm{d}\boldsymbol{V}\mathrm{d}I, \\ \boldsymbol{Q}_r\cdot\boldsymbol{n} &= \int I\boldsymbol{C}\cdot\boldsymbol{n}f_w\mathrm{d}\boldsymbol{V}\mathrm{d}I. \end{aligned} \tag{25}$$

From (17), f_w contains the distribution of the incident molecules $f^- = f_0 + f_1$ and the one of the reflected molecules f^+ that is calculated from (20) based on the kernel (23). Since the specular reflection does not contribute to the energy exchange in gas-surface interaction, the diffuse reflection part of f^+ is only considered, which is given by

$$f^+_{diff} = f_0(\boldsymbol{V}, T_w)\frac{\alpha_0}{2Z}\sqrt{\frac{T}{T_w}}\left[Z+1+\frac{T_t}{T}(Z-1)\right]. \tag{26}$$

Substituting (24) and (26) into (25), we obtain the expressions for the heat fluxes in the normal direction at the wall

$$\begin{aligned} \boldsymbol{Q}_t\cdot\boldsymbol{n} = & \frac{\alpha_0 n k_B^{3/2}}{Z(2\pi mT)^{1/2}}\left[\Big(T_w(T_t+T)+T(T-3T_t)\Big)Z\right. \\ & \left.-(T-T_t)(3T-T_w)\right] \\ & -\frac{\alpha_0}{24Zm}\left[\boldsymbol{n}\cdot\Big(-2m\left(Z\boldsymbol{Q}_t+\boldsymbol{Q}'-\boldsymbol{Q}_t\right)+15\mu Zk_B\nabla T\Big)\right], \\ \boldsymbol{Q}_r\cdot\boldsymbol{n} = & \frac{\alpha_0 n k_B^{3/2}}{4Z(2\pi mT)^{1/2}}\Big\{d\Big[T(Z+1)+T_t(Z-1)\Big](T_w-T) \\ & -6T(Z-1)(T-T_t)\Big\} \\ & +\frac{\alpha_0}{8Zm}\boldsymbol{n}\cdot\left[4m\left(Z\boldsymbol{Q}_r+\boldsymbol{Q}''-\boldsymbol{Q}_r\right)-2d\mu Zk_B\nabla T\right]. \end{aligned} \tag{27}$$

We denote $\Delta T_t = T_t - T_w$, $\Delta T_r = T_r - T_w$ as the jumps of the translational and rotational temperatures, respectively, and write the heat fluxes in terms of the Eucken factors (11) and the temperature gradient as

$$\boldsymbol{Q}_t\cdot\boldsymbol{n} = -\frac{3k_B\mu f_t}{2m}\frac{\partial T}{\partial n}, \quad \boldsymbol{Q}_r\cdot\boldsymbol{n} = -\frac{dk_B\mu f_r}{2m}\frac{\partial T}{\partial n}. \tag{28}$$

The correlations between the temperature jumps and the temperature gradient can be obtained as

$$\begin{aligned} \frac{\mu}{p}\left(\frac{2k_BT_w}{m}\right)^{1/2}\frac{\partial T}{\partial n} &= \frac{4\left[(Z-1)d+3Z\right]\alpha_0\Delta T_t+4d\alpha_0\Delta T_r}{3\sqrt{\pi}Z(d+3)\left[f_t+\frac{1}{6}\Big(dA_{tr}f_r+3(A_{tt}-1)f_t-5\Big)\right]}, \\ \frac{\mu}{p}\left(\frac{2k_BT_w}{m}\right)^{1/2}\frac{\partial T}{\partial n} &= \frac{3d\alpha_0\Delta T_t+d\left[3(Z-1)d+dZ\right]\alpha_0\Delta T_r}{\sqrt{\pi}Z(d+3)\left[df_r+\frac{1}{2}\alpha_0\Big(d(A_{rr}-1)f_r-d+3A_{rt}f_t-1\Big)\right]}. \end{aligned} \tag{29}$$

Note that the terms of $\Delta T_{t/r}$ with orders higher than one have been neglected in (29). The TJCs related to the translational, rotational and total temperatures, denoting as $\zeta^*_{T_t}$, $\zeta^*_{T_r}$ and ζ^*_T, respectively, are eventually solved as

$$\begin{aligned} \zeta^*_{T_t} &= \frac{2-\alpha_0}{\alpha_0}\frac{\sqrt{\pi}\left[3f_t\Big(Z(d+3)-3\Big)-4df_r\right]}{8(d+3)(Z-1)}, \\ \zeta^*_{T_r} &= \frac{2-\alpha_0}{\alpha_0}\frac{\sqrt{\pi}\left[-9f_t+4f_r\Big(Z(d+3)-d\Big)\right]}{8(d+3)(Z-1)}, \\ \zeta^*_T &= \frac{2-\alpha_0}{\alpha_0}\frac{\sqrt{\pi}\Big(9f_t+4df_r\Big)}{8(d+3)}. \end{aligned} \tag{30}$$

When $d = 0$, $f_t = 2.5$, $f_r = 0$ and $Z \to \infty$, the system approaches the limit of monatomic gases, and (30) gives

$$\zeta_T^* = \zeta_{T_t}^* = \frac{15\sqrt{\pi}}{16}\frac{2-\alpha_0}{\alpha_0}, \quad \zeta_{T_r}^* = 0, \tag{31}$$

where ζ_T^* is reduced to the estimation (2), providing $\gamma = 5/3$ and $Pr = 2/3$.

The temperature jump coefficients are plotted in Figure 2 for fully-diffuse gas surface interaction. From (30), we can have some simple observations:

1. Each of the three TJCs corresponding to the translational, rotational and overall temperatures could be quit different from the other twos for a certain gas species.

2. The values of TJCs varies with f_t and f_r even when the total thermal conductivity is fixed; although f_t and f_r are determined by the thermal relaxation rates A_{ij} from (9) and (11), the value of any individual A_{ij} does not influence the TJCs.

3. The rotational collision number Z affect the translational and rotational TJCs, where the two TJCs approaches infinity (physically impossible) as $Z \to 1$; however the overall TJC has no dependence on it.

4. For the Maxwell's boundary condition, the accommodation coefficient changes the values of TJCs through the same factor $(2-\alpha_0)/\alpha_0$.

The analytical formulations (30) are derived by making a truncation in the velocity-energy distribution functions up to the first order of Chapman-Enskog expansion, i.e., when the Navier-Stokes equations are valid. It is worth noting that the Navier-Stokes equations cannot resolve the Knudsen layer, which give additional contributions to the temperature jump, see the dash-dotted line and the dash line in Figure 1. The assumption of the first-order Chapman-Enskog distribution function may induce large error, e.g., an error of about 15% for monatomic gases[4]. In the following sections, we will numerically investigate the temperature jump based on the kinetic description that accounts for all the rarefied effects, and calculate the TJC and Knudsen layer function by comparing the kinetic solution inside the Knudsen layer to the outer Navier-Stokes solution.

IV. FORMULATIONS FOR NUMERICAL SOLUTION

We calculate the temperature jump problem via the heat conduction in a dilute molecular gas confined between two parallel plates located at $X_1 = 0$ and $X_1 = L$, respectively. The plate fixed at $X_1 = 0$ maintains at a temperature $T_0 + \Delta T/2$, while the other plate has a temperature $T_0 - \Delta T/2$, so that T_0 is a reference temperature and ΔT is the temperature difference between the two plates. We will investigate the kinetic effects introduced by the plates under the follow assumptions:

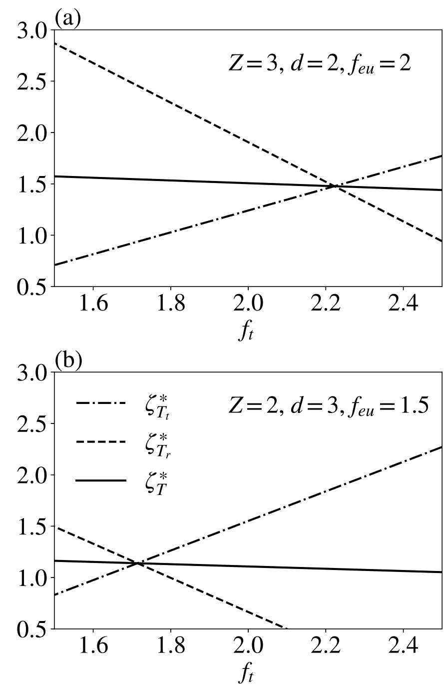

FIG. 2. The analytical estimation of TJCs under fully-diffuse gas-surface interaction (30) with $\alpha_0 = 1$: influence of the Eucken factors, f_t varies from 1.5 to 2.5. (a) $Z = 3$, $d = 2$ and $f_{eu} = 2$; (b) $Z = 2$, $d = 3$ and $f_{eu} = 1.5$.

1. $Kn \ll 1$, such that the Navier-Stokes description, i.e., the Laplace equation $\partial^2 T/\partial X_1^2 = 0$ subject to the boundary condition (1) is valid; the kinetic effects are only important within the Knudsen layer and can be quantified by the Knudsen layer function, which vanishes rapidly away from the boundary with length scale of variation of the order of Kn.

2. $\Delta T \ll T_0$, such that variations of the result through the temperature dependence of transport coefficients are negligible. The weakly disturbed system can be linearized around the reference equilibrium state at rest with density ρ_0 and temperature T_0

A. Linear governing system

We have present the kinetic description in §II. To improve computational efficiency, two reduced velocity distribution functions $G(\hat{t}, \boldsymbol{X}, \boldsymbol{V}) = \int_0^\infty f \mathrm{d}I$ and $R(\hat{t}, \boldsymbol{X}, \boldsymbol{V}) = \int_0^\infty I f \mathrm{d}I$ are introduced to eliminate the dependence on I. According to the assumption (ii), the reduced distribution functions can be linearized around global equilibrium state as $G = n_0(E_0 + h_0)/v_m^3$ and $R = n_0 k_B T_0 (d/2 E_0 + h_1)/v_m^3$, where $E_0 = \pi^{-3/2}\exp(-\boldsymbol{v}^2)$ is the equilibrium distribution function, $\boldsymbol{v} = \boldsymbol{V}/v_m$ and $v_m = \sqrt{2k_B T_0/m}$ is the most probable molecular speed. Let us further denote: $\boldsymbol{X} = L\boldsymbol{x}$, $n = n_0(1+\rho)$, $\boldsymbol{U} = v_m \boldsymbol{u}$, $T_t = T_0(1+\theta_t)$, $T_r = T_0(1+\theta_r)$, $(\boldsymbol{Q}_t, \boldsymbol{Q}_r, \boldsymbol{Q}', \boldsymbol{Q}'') = n_0 k_B T_0 v_m (\boldsymbol{q}_t, \boldsymbol{q}_r, \boldsymbol{q}', \boldsymbol{q}'')$, $(\hat{t}, \hat{\tau}) = L/v_m(t, \tau)$, $T = T_0(1+\theta)$ with $\theta = (3\theta_t + d\theta_r)/(3+d)$, $p_t = n_0 k_B T_0(1+\rho+\theta_t)$ and $p = n_0 k_B T_0 (1+\rho+\theta)$. Finally, if we introduce $h_2 = h_1 - dh_0/2$, the evolution of the linear system is eventually described by h_0 and h_2, whose governing equations are

$$\begin{aligned}\frac{\partial h_0}{\partial t} + \boldsymbol{v}\cdot\frac{\partial h_0}{\partial \boldsymbol{x}} &= \mathscr{L}_0,\\ \frac{\partial h_2}{\partial t} + \boldsymbol{v}\cdot\frac{\partial h_2}{\partial \boldsymbol{x}} &= \mathscr{L}_2,\end{aligned} \tag{32}$$

where

$$\begin{aligned}\mathscr{L}_0 &= \mathscr{L}_S + \frac{E_0}{Z\tau}\left[(\theta-\theta_t)\left(\boldsymbol{v}^2-\frac{3}{2}\right) + \frac{4(\boldsymbol{q}'-\boldsymbol{q}_t)\cdot\boldsymbol{v}}{15}\left(\boldsymbol{v}^2-\frac{5}{2}\right)\right],\\ \mathscr{L}_2 &= \frac{1}{\tau}\left(\frac{d}{2}E_0\theta_r - h_2\right) + \frac{dE_0}{2Z\tau}(\theta-\theta_r) + \frac{2E_0}{Z\tau}\boldsymbol{q}''\cdot\boldsymbol{v},\end{aligned} \tag{33}$$

with

$$\begin{aligned}\mathscr{L}_S = \frac{1}{\tau}\Big\{E_0\Big[\rho + 2\boldsymbol{u}\cdot\boldsymbol{v} + \theta_t\left(\boldsymbol{v}^2-\frac{3}{2}\right)\\ + \frac{4\boldsymbol{q}_t\cdot\boldsymbol{v}}{15}\left(\boldsymbol{v}^2-\frac{5}{2}\right)\Big] - h_0\Big\}.\end{aligned} \tag{34}$$

The dimensionless mean relaxation time, which has the order of the Knudsen number, is expressed as

$$\tau = \frac{2Kn}{\sqrt{\pi}} = \frac{\mu(T_0)}{n_0 L}\sqrt{\frac{2}{mk_B T_0}}. \tag{35}$$

The perturbations of macroscopic flow properties from the global equilibrium state are calculated from the velocity moments of h_0 and h_2

$$\begin{aligned}[\rho, \boldsymbol{u}, \theta_t, \boldsymbol{q}_t] &= \int\left[1, \boldsymbol{v}, \frac{2}{3}v^2 - 1, \boldsymbol{v}\left(v^2 - \frac{5}{2}\right)\right]h_0 \mathrm{d}\boldsymbol{v},\\ [\theta_r, \boldsymbol{q}_r] &= \int\left[\frac{2}{d}, \boldsymbol{v}\right]h_2 \mathrm{d}\boldsymbol{v}.\end{aligned} \tag{36}$$

We have mentioned that the kinetic model is reduced to the Shakhov model for monatomic gases in the limit of $Z \to \infty$. However, it may bring errors due to the fact that a velocity-independent relaxation time τ is used. To improve the model accuracy, Wu proposed to recover the realistic relaxation time by replacing the elastic collision part $\mathscr{L}_S$ with the Boltzmann collision operator[33]

$$\begin{aligned}\mathscr{L}_B = \iint B\Big[E_0(\boldsymbol{v}')h_0(\boldsymbol{v}'_*) + E_0(\boldsymbol{v}'_*)h_0(\boldsymbol{v}')\\ - E_0(\boldsymbol{v})h_0(\boldsymbol{v}_*) - E_0(\boldsymbol{v}_*)h_0(\boldsymbol{v})\Big]\mathrm{d}\Omega\mathrm{d}\boldsymbol{v}_*,\end{aligned} \tag{37}$$

where B is the collision kernel, $\boldsymbol{v}$, $\boldsymbol{v}_*$, $\boldsymbol{v}'$, and $\boldsymbol{v}'_*$ are the pre/post velocities of a collision pair, and Ω is the solid angle. The collision kernel is determined by the intermolecular potential. In this paper, we employ the inverse power law, where the shear viscosity is a single power-law function of temperature, i.e., $\mu \propto T_t^{\omega}$ with ω the viscosity exponent.

Under the Maxwell's boundary condition with a constant accommodation coefficient, the perturbed distribution functions at the walls ($x_1 = 0$ or 1) are determined as

$$\begin{aligned}h_0(\boldsymbol{v}) =& \alpha_0 E_0\Big[\pm\Delta\theta\left(\boldsymbol{v}^2-2\right)\\ &- 2\sqrt{\pi}\int_{\boldsymbol{v}'\cdot\boldsymbol{n}<0}\boldsymbol{v}'\cdot\boldsymbol{n}h_0(\boldsymbol{v}')\mathrm{d}\boldsymbol{v}'\Big]\\ &+ (1-\alpha_0)h_0(\boldsymbol{v}-2(\boldsymbol{v}\cdot\boldsymbol{n})\boldsymbol{n}),\\ h_2(\boldsymbol{v}) =& \pm\alpha_0 E_0\frac{d}{2}\Delta\theta + (1-\alpha_0)h_2(\boldsymbol{v}-2(\boldsymbol{v}\cdot\boldsymbol{n})\boldsymbol{n}),\end{aligned} \tag{38}$$

where $\Delta\theta = \Delta T/T_0$ is the perturbation of wall temperature.

B. Determination of TJC and Knudsen layer function

In order to avoid overlap of the two Knudsen layers adjacent to the plates, we set a small Knudsen number thus $\tau = 0.01$. The discrete velocity method is employed to deterministically solve the kinetic equations (32), where the steady-state solution is obtained using the general synthetic iterative scheme[40–42] that is developed by the authors to improve inefficiency and inaccuracy of the conventional iterative scheme for small-Knudsen-number flows. In the scheme, a set of synthetic equations governing the evolution of macroscopic flow properties are simultaneously solved with the kinetic equations, which help accelerate the evolution of distribution functions. The kinetic equations in turn provide high-order terms for the constitutive relations in the macroscopic equations and the boundary condition as well. It has been rigorously proven that the scheme can achieve fast convergence, i.e., obtain steady-state solution within dozen of iterations over the whole range of Knudsen numbers, retain accuracy in the high Knudsen number region and asymptotically preserve the Navier-Stokes solution on very coarse spatial grid when $Kn \to 0$. Hence it is efficient and accurate to simulate the current multiscale problem, possessing hydrodynamic scale in the bulk region and kinetic scale in the Knudsen layer. The details of the numerical scheme for linear flows of molecular gases can be found in Ref.[42]. We will omit the description in the present paper and leave some remarks on the accuracy of the computation in Appendix.

The TJC is calculated from the linear fitting of the temperature profile, named θ_{NS}, in the bulk region ($x_1 \in [0.3, 0.7]$), according to its definition (1) as

$$\zeta_T = -\frac{k+\Delta\theta}{2k\tau}, \tag{39}$$

where k is the slope coefficient in the linear fitting

$$\theta_{NS}(x_1) = k\left(x_1 - \frac{1}{2}\right)\Delta\theta. \tag{40}$$

TABLE I. Temperature jump coefficient ζ_T in monatomic gases. The inverse law potential is consider with the viscosity component setting as $\omega = 0.5$ and $\omega = 1.0$.

ω	0.5	1.0
ζ_T	1.9321	2.0058
ζ_T from[9]	1.9194	-

The Knudsen lay function, i.e., defective temperature Θ, is obtained by comparing the kinetic solution and the linear fitting within the Knudsen layer

$$\Theta(x_1) = \frac{1}{k\tau\Delta\theta}\left(\theta_{NS} - \theta\right). \quad (41)$$

We will separately consider the TJC (Knudsen layer function) for the translational and rotational temperatures, which are denoted as ζ_{T_t} (Θ_t) and ζ_{T_r} (Θ_r), respectively in the following sections.

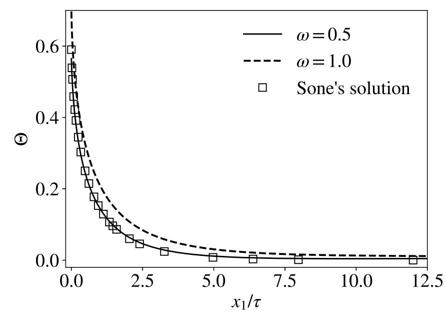

FIG. 3. Comparison of the Knudsen layer functions in monatomic gases. Lines are our results obtained by solving the linearized Boltzmann equation. Markers illustrates[9] results for hard-sphere molecules.

V. RESULTS AND DISCUSSIONS

We first present results in monatomic gases that are obtained by solving the linearized Boltzmann equation. The results will be compared to the data in the literature, to show the accuracy of our solutions. Then elaborate results and discussions will be given for molecular gases.

A. Temperature jump in monatomic gas

We consider two different cases, choosing $\omega = 0.5$ and $\omega = 1.0$, which correspond to the hard-sphere and Maxwellian molecular models. A more realistic potential will lead to a result between the two situations[43]. The boundary condition is fully-diffuse wall with $\alpha_0 = 1$ in (38). The obtained TJCs are listed in Table I, while the Knudsen layer functions are plotted in Figure 3. The solutions for hard-sphere molecules obtained by Sone[9] who used a finite different scheme to directly solve the linear Boltzmann equation, has also been included. Note that due to a different definition of normalization, Sone's original results are multiplied by 4/5 to make equivalent to our solutions. It is observed that our results have a good agreement to the reference data, where relative difference between the TJCs for $\omega = 0.5$ is about 0.67%. Just as that have been found in the literature, the temperature jump is not sensitive to the intermolecular potential: the TJC rises with a magnitude of 0.07 from the hard-sphere model to the Maxwell model; the maximum absolute difference in the Knudsen layer function is about 0.13.

B. Temperature jump in molecular gas

For reliable results, we need to determine the freely adjustable parameters in the kinetic model. A proper value for the rotational collision number can be obtained to recover the experimentally measured shear and bulk viscosities. However, it is difficult to determine the thermal relaxation rates from an experimental measurement of the thermal conductivity, since only the total conductivity is straightforwardly obtained. In this paper, we use the values of Z and A_{ij} extracted from the direct simulation Monet Carlo (DSMC) method. In the DSMC equipping with the variable-soft-sphere model[43] and the Borgnakke and Larsen [44] collision rule for molecular gases, the rotational collision number is the only factor that can modify the thermal relaxation rates once the shear viscosity and self-diffusivity are fixed; by monitoring the relaxation of heat fluxes in homogeneous systems, the correlations of A_{ij} against Z can be obtained[25]. It is shown that all the parameters A_{ij} are inversely proportional to the rotational collision number. By matching the total thermal conductivity, or equivalently $f_{eu} = 1.993$ at $T_0 = 300$ K measured in the Rayleigh-Brillouin scattering in rarefied gases[24], the parameters for nitrogen are given as: $Z = 2.667$, $A_{tt} = 0.786$, $A_{tr} = -0.201$, $A_{rt} = -0.059$, and $A_{rr} = 0.842$, resulting in $f_t = 2.365$ and $f_r = 1.435$. Considering that both the bulk viscosity and thermal conductivity are determined by the collision number in the DSMC, the given value of Z may not lead to the correct bulk viscosity.

We have shown that the molecular interaction in elastic collision does not significantly influence the TJC and the Knudsen layer function. Now we are investigating how the unique transport processes in molecular gases affect the temperature jump. We first consider the influence of the temperature relaxation (6) by changing the rotational collision number. The gas is nitrogen with $\omega = 0.74$, $d = 2$, $f_t = 2.365$ and $f_r = 1.435$ (or $A_{tt} = 0.786$, $A_{tr} = -0.201$, $A_{rt} = -0.059$, and $A_{rr} = 0.842$). We set three different values of Z as 1.0, 2.667 and 5.0. The boundary condition is set as fully-diffuse reflection. The obtained temperature jump coefficients are listed in Table II. It is found that the three TJCs have almost the same value of about 1.73, due to the fact that the translational, rotational and overall temperatures coincide in the bulk region, i.e., outside

TABLE II. Temperature jump coefficients in molecular gases with different rotational collision numbers Z. The other parameters are $d = 2$, $\omega = 0.74$, $A_{tt} = 0.786$, $A_{tr} = -0.201$, $A_{rt} = -0.059$, and $A_{rr} = 0.842$, thus $f_t = 2.365$, $f_r = 1.435$ and $f_{eu} = 1.993$. Fully-diffuse gas-wall interaction is considered.

Z	1.0	2.667	5.0
ζ_{T_t}	1.7300	1.7303	1.7305
ζ_{T_r}	1.7300	1.7302	1.7303
ζ_T	1.7300	1.7303	1.7304

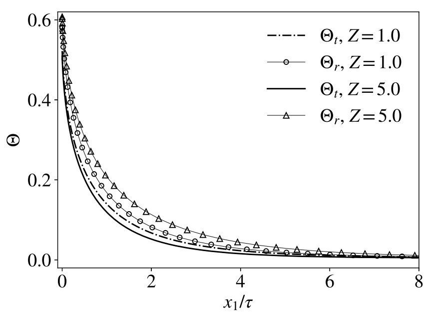

FIG. 4. The Knudsen layer functions for the translational and the rotational temperatures when $Z = 1.0$ and $Z = 5.0$. The other parameters are $d = 2$, $\omega = 0.74$, $A_{tt} = 0.786$, $A_{tr} = -0.201$, $A_{rt} = -0.059$, and $A_{rr} = 0.842$, thus $f_t = 2.365$, $f_r = 1.435$ and $f_{eu} = 1.993$. Fully-diffuse gas-wall interaction is considered.

of the Knudsen layer. The rotational collision number Z has hardly any influence on the TJC. The translational and rotational Knudsen layer functions for $Z = 1.0$ and $Z = 5.0$ are plotted in Figure 4, which demonstrates that the rarefied effect in the Knudsen layer leads to the deviations between the translational and internal temperatures. When $Z = 1.0$, i.e., inelastic collisions that exchange translational and internal energies frequently take place, Θ_t and Θ_r are close, while as Z increases to 5.0, i.e., the probability for inelastic collisions becomes smaller, the discrepancy between Θ_t and Θ_r enlarges. However, the variation is not significant.

Then we study the influence of thermal relaxations (7) by changing the relaxation rates and retaining $Z = 2.667$. The thermal conductivities will vary with A_{ij}, therefore in order to make duly comparisons, the total Eucken factor $f_{eu} = 1.993$ is kept as the experimental value for nitrogen at $T_0 = 300$ K. When we alter the values of f_t and f_r, the cross terms A_{tr} and A_{rt} are also fixed, while the diagonal terms A_{tt} and A_{rr} will change correspondingly. Figure 5(a) displays the TJCs against the translational Eucken factor, where the three lines relate to the three groups of cross terms: $A_{tr} = A_{rt} = 0.0$ without cross exchanges; $A_{tr} = -0.201$ and $A_{rt} = -0.059$ the ones extracted from the DSMC; $A_{tr} = -1.005$ and $A_{rt} - 0.295$ that are 5 times larger, in magnitude, than the previous group, representing intensified cross exchanges. Note that the TJCs for the different temperatures are almost the same, thus only the values of ζ_T are plotted. The TJC first falls and then slightly rises as f_t increases (or f_r decreases), and the minimum value that is about 1.72 appears when f_t is around $2.2 \sim 2.25$. Large values of TJC occur when f_t (f_r) is relative small (large). When f_t varies from 1.5 to 2.5, the largest TJC is about 110%∼115% of the minimum one. For a fixed group of f_t and f_r, the TJC slightly changes with the thermal relaxation rates, where the variation in magnitude is smaller than 0.1. The Knudsen layer functions are plotted in Figure 5(b) for $A_{tr} = -0.201$ and $A_{rt} = -0.059$. It is shown that, when $f_t = 1.5$ and $f_r = 2.733$, the translational Knudsen layer function Θ_t is larger than the rotational Θ_r, which implies that T_t in the Knudsen layer deviates more from the Navier-Stokes solution; while when f_t increases to 2.5 and f_r reduces, the situation reverses and now Θ_r is larger. The two Knudsen layer functions meet at around $f_t \simeq 2.20$, which corresponds to that when the minimum temperature jump coefficient emerges.

Compared to monatomic gases, the TJC in molecular gases is generally smaller.

C. The minimum TJC

We have shown that for a selected gas species with a certain internal degree of freedom and a fixed total thermal conductivity, the values of TJC and Knudsen layer function depend on the relative quantity of the translational contribution in the total thermal conductivity to the internal one. When the translational contribution f_t is relatively larger, the translational Knudsen layer function is smaller than the internal one, i.e., the translational temperature is closer to the extrapolated Navier-Stokes solution in the Knudsen layer; the situation reverses when the internal contribution becomes relatively larger. A minimum TJC can be found when the translational and internal Knudsen layer functions overlap; the larger the differences between the translational and rotational Knudsen layer functions or the translational and internal components of the total thermal conductivity, the larger the TJC.

We can give an estimation at which value of f_t the minimum TJC appears under the classical Maxwell's gas-surface interaction. Since the translational and internal Knudsen functions are coincident, the analytical TJCs (30) that exclude the effect from the Knudsen layer, should be equal to each other, see the dotted dash line in Figure (1), corresponding to the crossover points of the three lines in 2(a) and (b). Therefore from (30), we find the minimum TJC emerges when

$$f_t = \frac{4}{3} f_r = \frac{4(3+d)}{3(4+d)} f_{eu}, \qquad (42)$$

which is independent on the rotational collision number and the accommodation coefficient. This is further confirmed from the numerical results illustrated in Figure 6.

D. Correction to the analytical TJC

Comparing the numerical results of the TJC presented in this section to the ones obtained from the analytical formu-

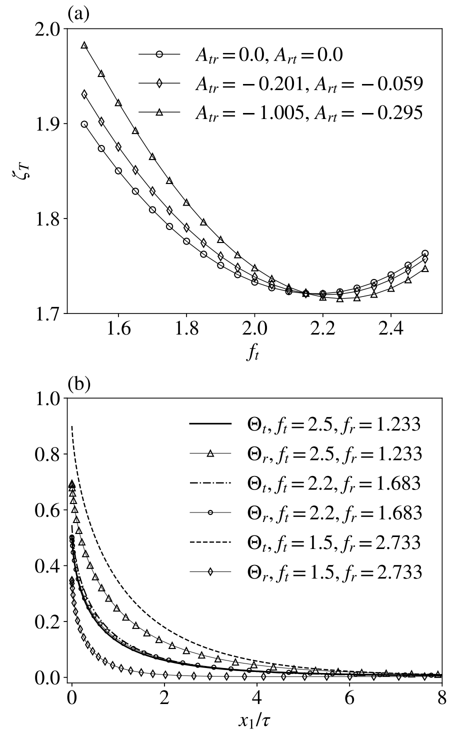

FIG. 5. Influence of the translational and rotational Eucken factors when the total one is fixed $f_{eu}=1.993$: (a) Temperature jump coefficient displaying the influence of three different groups of A_{tr} and A_{rt}. (b) Knudsen layer functions displaying the influence when $A_{tr}=-0.201$ and $A_{rt}=-0.059$. The other gas parameters are $Z=2.667$, $d=2$ and $\omega=0.74$. Fully-diffuse gas-wall interaction is considered.

lations given in § III, we can find that the estimate (30), in which the contribution from the Knudsen layer to the temperature jump has been excluded, possesses large errors. The main errors are:

1. The rotational collision number may have strong effect on the value of the analytical translational and internal TJCs, making them deviate a lot from the analytical overall TJC. However, the actual translational, internal as well as overall TJCs are almost identical due to the fact that the three temperatures overlap in the bulk region at small Knudsen numbers. The actual TJC is independent on the rotational collision number. Although the analytical overall TJC has this feature, it is much smaller than the actual TJC.

2. Under the classical Maxwell's boundary condition with a constant accommodation coefficient and for a certain

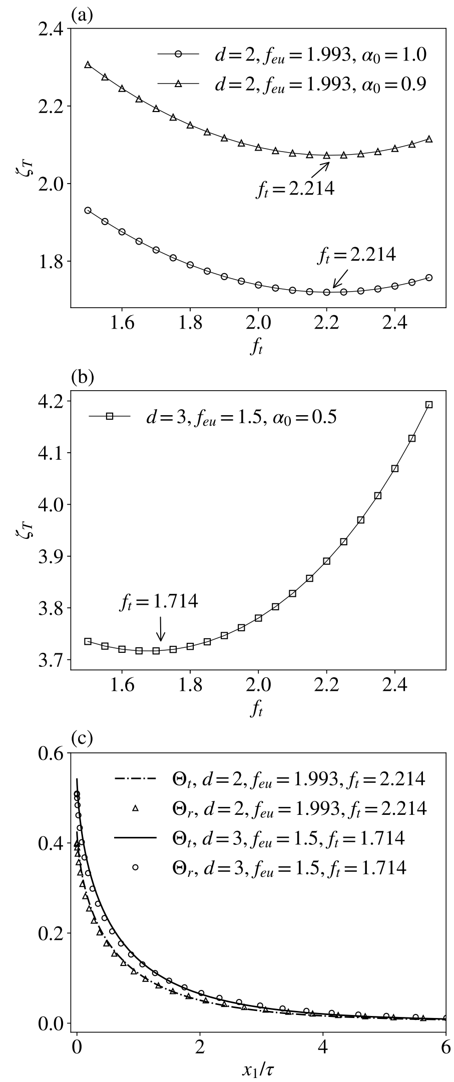

FIG. 6. Under the classical Maxwell's boundary condition with a constant accommodation coefficient, a minimum TJC can be found when the translational and internal components f_t and f_r vary but the total Eucken factor f_{eu} is fixed. (a)-(b) The value of f_t at which the minimum TJC appears is about $f_t=\frac{4(3+d)}{3(4+d)}f_{eu}$ that does not depend on the rotational collision number Z and the accommodation coefficient α_0; (c) The Knudsen layer functions of the translational and internal temperatures are coincident at the minimum TJC. For cases of $d=2$ and $f_{eu}=1.993$, we have set $Z=2.667$, $A_{tr}=-0.201$ and $A_{rt}=-0.059$. For cases of $d=3$ and $f_{eu}=1.5$, we have set $Z=3$ and $A_{tr}=A_{rt}=0.0$. In (c) $\alpha_0=1$.

value of total Eucken factor, the analytical formulation cannot reproduce the trend of the variation of TJC against the translational Eucken factor, that is the TJC first falls to a minimum value and then rises.

To correct the analytical estimation, we propose a new formulation for the TJC in molecular gases, read as

$$\zeta_T = \frac{2-\alpha_0}{\alpha_0}(1+0.1621\alpha_0)\frac{\sqrt{\pi}}{8}\left(\frac{4(3+d)}{4+d}f_{eu}+\left|\frac{4}{4+d}f_{eu}-\frac{3}{3+d}f_t\right|\right), \quad (43)$$

which is free of Z as well as the thermal relaxation rates A_{ij}, and can produce the minimum TJC at $f_t = \frac{4(3+d)}{3(4+d)}f_{eu}$. It can also be shown that this new formulation is reduced to (4) for monatomic gases when $d=0$ and $f_{eu}=f_t=\frac{5}{2}$. The comparisons between the new formulated TJC and the numerical solutions are plotted in Figure 7. The formulation shows high accuracy especially around the minimum values, while the deviation becomes slightly larger when TJC is getting higher. This can be explained by the neglect of higher order terms of $\Delta T_{t/r}$ in (29), which leads to linear dependence of TJC on the Eucken factors. While it can be seen from Figure 7 that the numerical results of TJC show slight nonlinear dependence on f_t. Nevertheless, for all the considered cases, the relative differences between the TJCs calculated from (43) and the numerical ones are not larger than 5.78%.

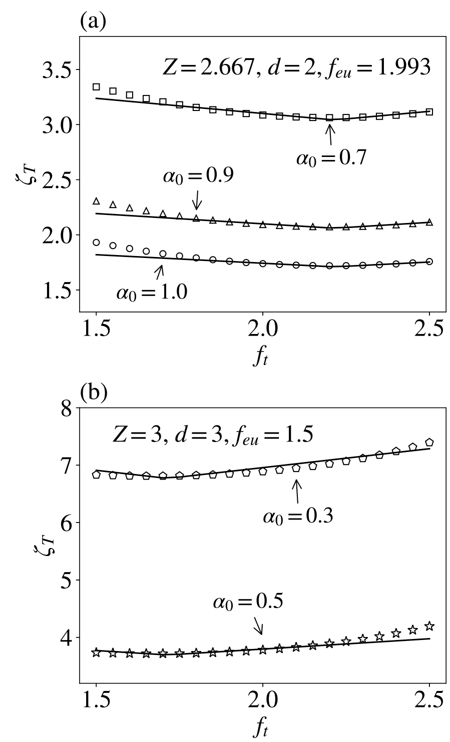

FIG. 7. A new formulation (43) is proposed to estimate the TJC in molecular gases under the classical Maxwell's gas-surface interaction with a constant accommodation coefficient α_0. Comparison between the new estimated (solid lines) and numerical (markers) results: (a) $d=2$, $Z=2.667$, $f_{eu}=1.993$, $A_{tr}=-0.201$, and $A_{rt}=-0.059$; (b) $d=3$, $Z=3$, $f_{eu}=1.5$, $A_{tr}=A_{rt}=0$.

VI. CONCLUSIONS

We have investigated the temperature jump problem in rarefied molecular (diatomic and polyatomic) gases with excited rotational energy, on the base of a kinetic model that is capable to realize the temperature relaxation described by the Landau relation and the general thermal relaxation predicted by the Wang-Chang Uhlenbeck equation. In the kinetic model, the relaxation rates of these unique transport processes in molecular gases can be freely adjustable, the influences of which on the temperature jump have been separately investigated. Analytical estimations of the temperature jump coefficient subject to the Maxwell's gas-surface interaction with a constant accommodation coefficient have been obtained by assuming a first-order Chapman-Enskog velocity-energy distribution function. The analytical TJCs are functions of the accommodation coefficient, the internal degree of freedom, the rotational collision number, as well as the Eucken factor and its translational and internal components. Due to the fact that the Knudsen layer cannot be resolved from the first-order truncated distribution function, the analytical estimations may possess larger errors. The temperature jump coefficient and the Knudsen layer function have been numerical calculated by directly solving the kinetic model for the one-dimensional steady conductive problem. Some conclusions can be obtained from the numerical results:

1. Compared to the one of a monatomic gas, the temperature jump coefficient is general smaller in molecular gases, where energy-exchange between translational and internal motions occurs.
2. The temperature jump coefficients related to the translational, internal and overall temperatures are coincident due to the fact that the three temperatures overlap in the bulk region when the Knudsen number is small. But

TABLE III. Computations are carried out on different grid systems to find converged results of the jump coefficient ζ_T.

Case	$N=64$ $N_v=96\times24\times24$ $N_f=48\times24\times24$	$N=64$ $N_v=48\times24\times24$ $N_f=24\times24\times24$	$N=64$ $N_v=96\times48\times24$ $N_f=48\times24\times24$	$N=128$ $N_v=96\times24\times24$ $N_f=48\times24\times24$
#1	1.7307	1.7705	1.7339	1.7302
#2	1.8994	1.9292	1.9017	1.8994
#3	1.7638	1.8058	1.7672	1.7633
#4	1.9834	2.0065	1.9853	1.9828
#5	1.7479	1.7888	1.7513	1.7474

the corresponding Knudsen layers may be quit different due to the rarefaction effect.

3. The intermolecular potential for the elastic collisions has a limited influence on the temperature jump.

4. The temperature jump coefficient is almost independent on the rotational collision number. However, the difference between the translational and internal Knudsen layer functions enlarges as the rotational collision number increases, although the variation is not significant.

5. The thermal relaxation processes significantly affect the temperature jump. The value of the temperature jump coefficient is determined by the relative quantity of the translational components in the total thermal conductive to the rotational one. For a certain gas species with a fixed total Eucken factor, the temperature jump coefficient and the Knudsen layer functions vary with the translational Eucken factor. A minimum value of the temperature jump coefficient emerges when the Eucken factors are $f_t=\frac{4}{3}f_r=\frac{4(3+d)}{3(4+d)}f_{eu}$, where the translational and internal Knudsen layer functions are coincident.

Based on the numerical results, a new formulation has been proposed to estimate the temperature jump coefficient under the classical Maxwell's boundary condition, which is a function of the internal degree of freedom, the total Eucken factor and its translational component, and the constant accommodation coefficient. The formulation is reduced to the one for monatomic gases in the limit when the translational-rotational energy exchange vanishes.

ACKNOWLEDGMENTS

This work has been financially supported by the National Natural Science Foundation of China under the grant number 12172162.

DATA AVAILABILITY STATEMENT

The data that support the findings of this study are available from the corresponding author upon reasonable request.

Appendix A: On the accuracy of the numerical results

In this section, we present some analyses about the accuracy of our numerical results. To find the solution of the heat conduction problem, the kinetic model equation (32) is solved by the discrete velocity method combining with the general synthetic iterative scheme. The spatial derivatives in the governing equations are approximated by the 4th-order discontinuous Galerkin method on one-dimensional domain partitioned by N linear segments. The cell size is refined near the solid plates. The integrals in the molecular velocity space are approximated by the first-order quadrature rule. $N_v=N_v^1\times N_v^2\times N_v^3$ discrete velocities are allocated over a truncated domain of $[-6,6]^3$, where v_1 is discretized by non-uniform nodes with refinement around $v_1=0$, while v_2 and v_3 are discretized by uniform nodes. The means to partition the spatial and velocity spaces can be found in Ref.[42], see equations (43) and (47) there. The linearized Boltzmann collision operator is evaluated by the fast spectral method, using $N_f=N_f^1\times N_f^2\times N_f^3$ uniform frequencies. The details of the fast spectral method can be found in Ref.[45,46]. When conducting the iterative scheme to find the steady-state solution, the iteration terminates when the maximum residue in flow density, temperature and heat fluxes is smaller than 10^{-6}.

We carried out computations on different grid systems and confirmed that the obtained results are close to each other. The obtained temperature jump coefficients from different cases:

1. #1: $Z=2.667$, $f_t=2.365$, $f_{eu}=1.993$, $A_{tr}=-0.201$ and $A_{rt}=-0.059$;

2. #2: $Z=2.667$, $f_t=1.5$, $f_{eu}=1.993$, $A_{tr}=A_{rt}=0.0$;

3. #3: $Z=2.667$, $f_t=2.5$, $f_{eu}=1.993$, $A_{tr}=A_{rt}=0.0$;

4. #4: $Z=2.667$, $f_t=1.5$, $f_{eu}=1.993$, $A_{tr}=-1.005$, $A_{rt}=-0.295$;

5. #5: $Z=2.667$, $f_t=2.5$, $f_{eu}=1.993$, $A_{tr}=-1.005$, $A_{rt}=-0.295$;

are listed in Table III. The results presented in §V are obtained with $N=128$, $N_v=96\times24\times24$ and $N_f=48\times24\times24$.

Nomenclature	
$\boldsymbol{A}$	matrix of relaxation rates
$\boldsymbol{C}$	peculiar velocity
d	rotational degrees of freedom
$E_t,\ E_r$	equilibrium distribution of velocity and rotational energy
f	velocity-energy distribution function
f_0	equilibrium velocity-energy distribution function
f_1	perturbed distribution function
$f_t,\ f_r,\ f_{eu}$	translational, rotational and total Eucken factor
f_w	velocity-energy distribution at the wall
$f^+,\ f^-$	incident and reflected distribution function
$g_t,\ g_r$	reference velocity distribution functions
$G,\ R$	reduced velocity distribution functions
$h_0,\ h_1 m\ h_2$	dimensionless perturbed velocity distribution functions
I	molecular rotational energy
I'	incident molecular rotational energy
k	slope coefficient in the linear fitting of temperature
k_B	Boltzmann constant
Kn	Knudsen number
L	characteristic flow length
$\mathscr{L}_0,\ \mathscr{L}_2$	collision terms in the linear system
$\mathscr{L}_S$	relaxation approximation of elastic collision
$\mathscr{L}_B$	Boltzmann operator
m	molecular mass
n	number density
n_0	reference number density
$\boldsymbol{n}$	outward normal vector at the wall
$p_t,\ p_r,\ p$	translational, rotational and overall pressure
Pr	Prandtl number
$\boldsymbol{q}_t,\ \boldsymbol{q}_r$	dimensionless translational, rotational heat flux
$\boldsymbol{q}',\ \boldsymbol{q}''$	linear combinations of $\boldsymbol{q}_t$ and $\boldsymbol{q}_r$
$\boldsymbol{Q}_t,\ \boldsymbol{Q}_r$	translational and rotational heat flux
$\boldsymbol{Q}',\ \boldsymbol{Q}''$	linear combinations of $\boldsymbol{Q}_t$ and $\boldsymbol{Q}_r$
$\mathscr{R}$	reflection kernel
$\hat{t}, t$	time, dimensionless time
$T_t,\ T_r,\ T$	translational, rotational and overall temperature
T_0	reference temperature
T_e	linearly extrapolated temperature
T_w	wall temperature
$\boldsymbol{U}, \boldsymbol{u}$	bulk velocity, dimensionless velocity
$\boldsymbol{v}_m$	most probable molecular speed
$\boldsymbol{V}$	molecular translational velocity
$\boldsymbol{V}'$	incident molecular translational velocity
$\boldsymbol{X}, \boldsymbol{x}$	location, dimensionless location
Z	rotational collision number
α_0	accommodation coefficient
γ	specific heat ratio
$\delta\theta$	dimensionless perturbed wall temperature
$\Delta T_t,\ \Delta T_r$	translational and rotational temperatures jump
ζ_T	temperature jump coefficient
$\zeta^*_{T_t},\ \zeta^*_{T_r},\ \zeta^*_T$	translational, rotational and overall TJCs
Θ	Knudsen lay function (defective temperature)
$\theta_t,\ \theta_r,\ \theta$	dimensionless perturbed temperature
θ_{NS}	linear fitting of the temperature profile
$\kappa_t,\ \kappa_r,\ \kappa$	translational, rotational and total thermal conductivity
λ	mean free path
μ	shear viscosity
μ_b	bulk viscosity
ρ	dimensionless perturbed number density
$\hat{\tau}, \tau$	relaxation time, dimensionless relaxation time
ω	viscosity index

REFERENCES

[1] J. T. Lin and D. R. Willis, "Kinetic theory analysis of temperature jump in a polyatomic gas," The Physics of Fluids **15**, 31–38 (1972).

[2] F. Sharipov, "Data on the velocity slip and temperature jump on a gas-solid interface," Journal of Physical and Chemical Reference Data **40**, 023101 (2011).

[3] E. H. Kennard, *Kinetic Theory of Gases* (New York, 1938).

[4] H. Struchtrup, "Macroscopic transport equations for rarefied gas flows," in *Macroscopic Transport Equations for Rarefied Gas Flows: Approximation Methods in Kinetic Theory* (Springer Berlin Heidelberg, Berlin, Heidelberg, 2005) pp. 145–160.

[5] P. Bassanini, C. Cercignani, and C. Pagani, "Comparison of kinetic theory analyses of linearized heat transfer between parallel plates," International Journal of Heat and Mass Transfer **10**, 447 – 460 (1967).

[6] L. B. Barichello and C. E. Siewert, "The temperature-jump problem in rarefied-gas dynamics," European Journal of Applied Mathematics **11**, 353–364 (2000).

[7] F. Sharipov, "Application of the cercignani–lampis scattering kernel to calculations of rarefied gas flows. ii. slip and jump coefficients," European Journal of Mechanics - B/Fluids **22**, 133 – 143 (2003).

[8] S. K. Loyalka, "Temperature jump and thermal creep slip: Rigid sphere gas," Physics of Fluids A: Fluid Dynamics **1**, 403–408 (1989).

[9] Y. Sone, T. Ohwada, and K. Aoki, "Temperature jump and knudsen layer in a rarefied gas over a plane wall: Numerical analysis of the linearized boltzmann equation for hard-sphere molecules," Physics of Fluids A: Fluid Dynamics **1**, 363–370 (1989).

[10] S. Loyalka, "Slip and jump coefficients for rarefied gas flows: variational results for lennard-jones and n(r)-6 potentials," Physica A: Statistical Mechanics and its Applications **163**, 813 – 821 (1990).

[11] L. B. Barichello, A. C. R. Bartz, M. Camargo, and C. E. Siewert, "The temperature-jump problem for a variable collision frequency model," Physics of Fluids **14**, 382–391 (2002).

[12] C. Siewert, "The linearized boltzmann equation: a concise and accurate solution of the temperature-jump problem," Journal of Quantitative Spectroscopy and Radiative Transfer **77**, 417 – 432 (2003).

[13] S. K. Loyalka, "Momentum and temperature-slip coefficients with arbitrary accommodation at the surface," The Journal of Chemical Physics **48**, 5432–5436 (1968).

[14] S. K. Loyalka, "Temperature jump in a gas mixture," The Physics of Fluids **17**, 897–899 (1974).

[15] F. Sharipov and D. Kalempa, "Velocity slip and temperature jump coefficients for gaseous mixtures. iv. temperature jump coefficient," International Journal of Heat and Mass Transfer **48**, 1076 – 1083 (2005).

[16] G. A. Radtke, N. G. Hadjiconstantinou, S. Takata, and K. Aoki, "On the second-order temperature jump coefficient of a dilute gas," Journal of Fluid Mechanics **707**, 331–341 (2012).

[17] Y. Sone, *Molecular Gas Dynamics: Theory, Techniques, and Applications* (Birkhauser Basel, 2007).

[18] S. Takata, K. Aoki, M. Hattori, and N. G. Hadjiconstantinou, "Parabolic temperature profile and second-order temperature jump of a slightly rarefied gas in an unsteady two-surface problem," Physics of Fluids **24**, 032002 (2012).

[19] C. S. Wang-Chang and G. E. Uhlenbeck, "Transport phenomena in polyatomic gases, No. CM-681," Tech. Rep. (1951).

[20] M. Hattori, S. Kosuge, and K. Aoki, "Slip boundary conditions for the compressible navier-stokes equations for a polyatomic gas," Phys. Rev. Fluids **3**, 063401 (2018).

[21] P. Andries, P. Le Tallec, J.-P. Perlat, and B. Perthame, "The Gaussian-BGK model of Boltzmann equation with small Prandtl number," European Journal of Mechanics - B/Fluids **19**, 813–830 (2000).

[22] S. Brull and J. Schneider, Continuum Mechanics and Thermodynamics **20**, 489–508 (2009).

[23] G. V. Candler, "Rate effects in hypersonic flows," Annual Review of Fluid Mechanics **51**, 379–402 (2019).

[24] L. Wu, Q. Li, H. Liu, and W. Ubachs, "Extraction of the translational Eucken factor from light scattering by molecular gas," Journal of Fluid Mechanics **901**, A23 (2020).

[25] Q. Li, J. Zeng, W. Su, and L. Wu, "Uncertainty quantification in rarefied

dynamics of molecular gas: rate effect of thermal relaxation," Journal of Fluid Mechanics **917**, A58 (2021).

[26] T. F. Morse, "Kinetic model for gases with internal degrees of freedom," The Physics of Fluids **7**, 159–169 (1964).

[27] L. H. Holway, "New statistical models for kinetic theory: Methods of construction," The Physics of Fluids **9**, 1658–1673 (1966).

[28] D. R. Willis and B. B. Hamel, "Non-equilibrium effects in spherical expansions of polyatomic gases and gas mixtures," in *Rarefied Gas Dynamics*, Vol. I, edited by C. L. Brundin (Academic Press, New York, 1967) pp. 837–860.

[29] V. A. Rykov, "A model kinetic equation for a gas with rotational degrees of freedom," Fluid Dynamics , 959–966 (1975).

[30] P. Wang, W. Su, and L. Wu, "Thermal transpiration in molecular gas," Physics of Fluids **32**, 082005 (2020).

[31] Y. Dauvois, J. Mathiaud, and L. Mieussens, "An ES-BGK model for vibrational polyatomic gases," arXiv preprint arXiv:2007.02727 (2020).

[32] Z. Wang, H. Yan, Q. B. Li, and K. Xu, "Unified gas-kinetic scheme for diatomic molecular flow with translational, rotational, and vibrational modes," J. Comput. Phys. **350**, 237–259 (2017).

[33] L. Wu, C. White, T. J. Scanlon, J. M. Reese, and Y. Zhang, "A kinetic model of the Boltzmann equation for non-vibrating polyatomic gases," Journal of Fluid Mechanics **763**, 24–50 (2015).

[34] E. A. Mason and L. Monchick, "Heat conductivity of polyatomic and polar gases," The Journal of Chemical Physics **36**, 1622–1639 (1962).

[35] F. J. McCormack, "Kinetic equations for polyatomic gases: The 17-moment approximation," The Physics of Fluids **11**, 2533–2543 (1968).

[36] A. Eucken, "Über das Wärmeleitvermögen, die spezifische Wärme und die innere Reibung der Gase," Phys. Z **14**, 324 (1913).

[37] V. Lyusternik and R. Mustafaev, "Eucken factor and the role of internal degrees of freedom in polyatomic hydrocarbon molecule transfer effects," Journal of Engineering Physics **31**, 1211–1214 (1976).

[38] E. M. Shakhov, "Generalization of the krook kinetic relaxation equation," Fluid Dynamics **3**, 95–96 (1968).

[39] S. Chapman and T. G. Cowling, *The Mathematical Theory of Non-uniform Gases* (Cambridge University Press, 1970).

[40] W. Su, L. Zhu, P. Wang, Y. Zhang, and L. Wu, "Can we find steady-state solutions to multiscale rarefied gas flows within dozens of iterations?" Journal of Computational Physics **407**, 109245 (2020).

[41] W. Su, L. Zhu, and L. Wu, "Fast convergence and asymptotic preserving of the general synthetic iterative scheme," SIAM Journal on Scientific Computing **42**, B1517–B1540 (2020).

[42] W. Su, Y. Zhang, and L. Wu, "Multiscale simulation of molecular gas flows by the general synthetic iterative scheme," Computer Methods in Applied Mechanics and Engineering **373**, 113548 (2021).

[43] G. A. Bird, *Molecular Gas Dynamics and the Direct Simulation of Gas Flows* (Clarendon Press, 1994).

[44] C. Borgnakke and P. S. Larsen, "Statistical collision model for Monte Carlo simulation of polyatomic gas mixture," Journal of Computational Physics **18**, 405 – 420 (1975).

[45] L. Wu, C. White, T. J. Scanlon, J. M. Reese, and Y. Zhang, "Deterministic numerical solutions of the Boltzmann equation using the fast spectral method," Journal of Computational Physics **250**, 27 – 52 (2013).

[46] L. Wu, J. M. Reese, and Y. Zhang, "Solving the Boltzmann equation deterministically by the fast spectral method: application to gas microflows," Journal of Fluid Mechanics **746**, 53–84 (2014).

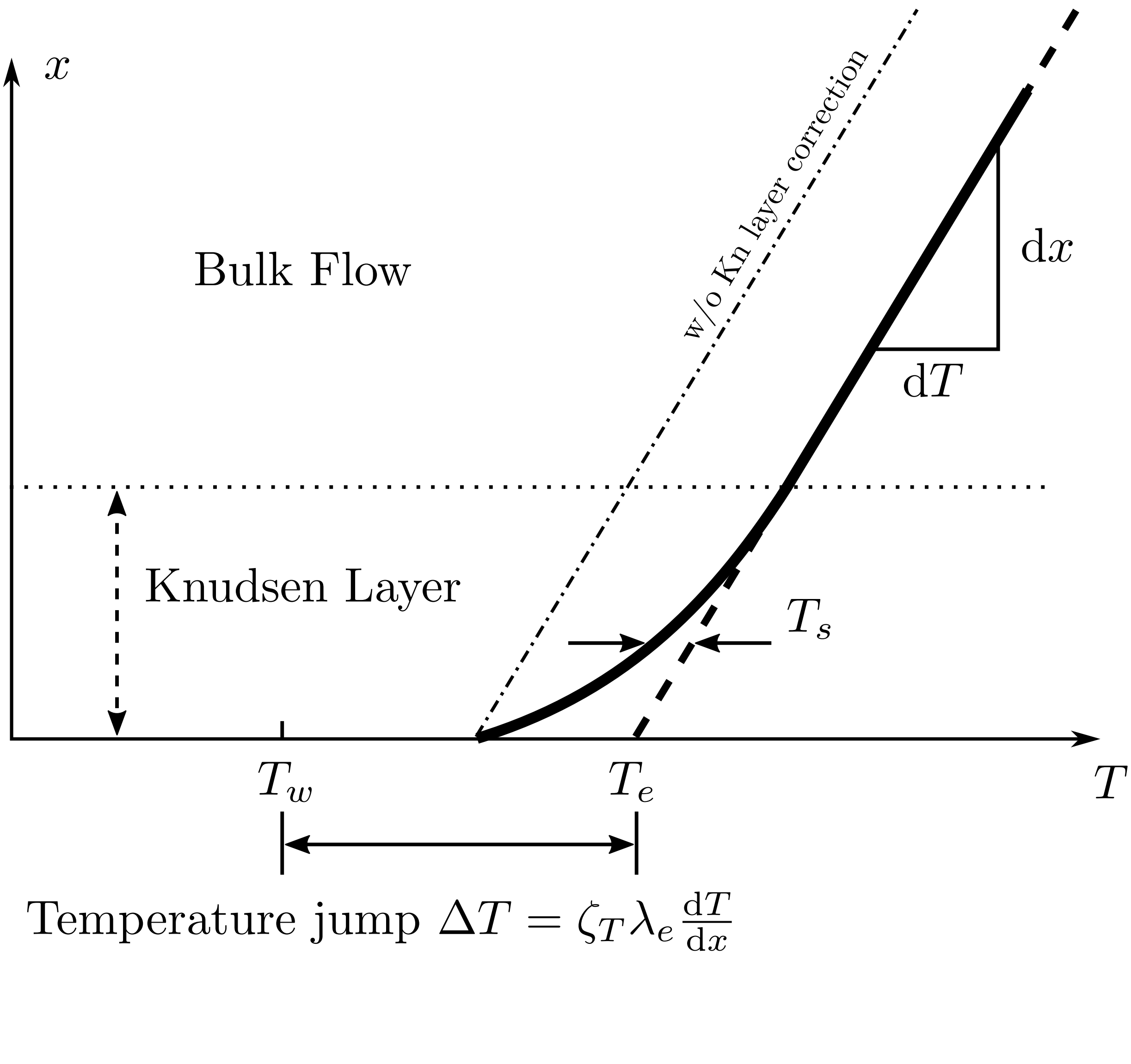
x
w/o Kn layer correction
Bulk Flow
dx
dT
Knudsen Layer
T_s
T_w
T_e
T
Temperature jump $\Delta T = \zeta_T \lambda_e \frac{\mathrm{d}T}{\mathrm{d}x}$

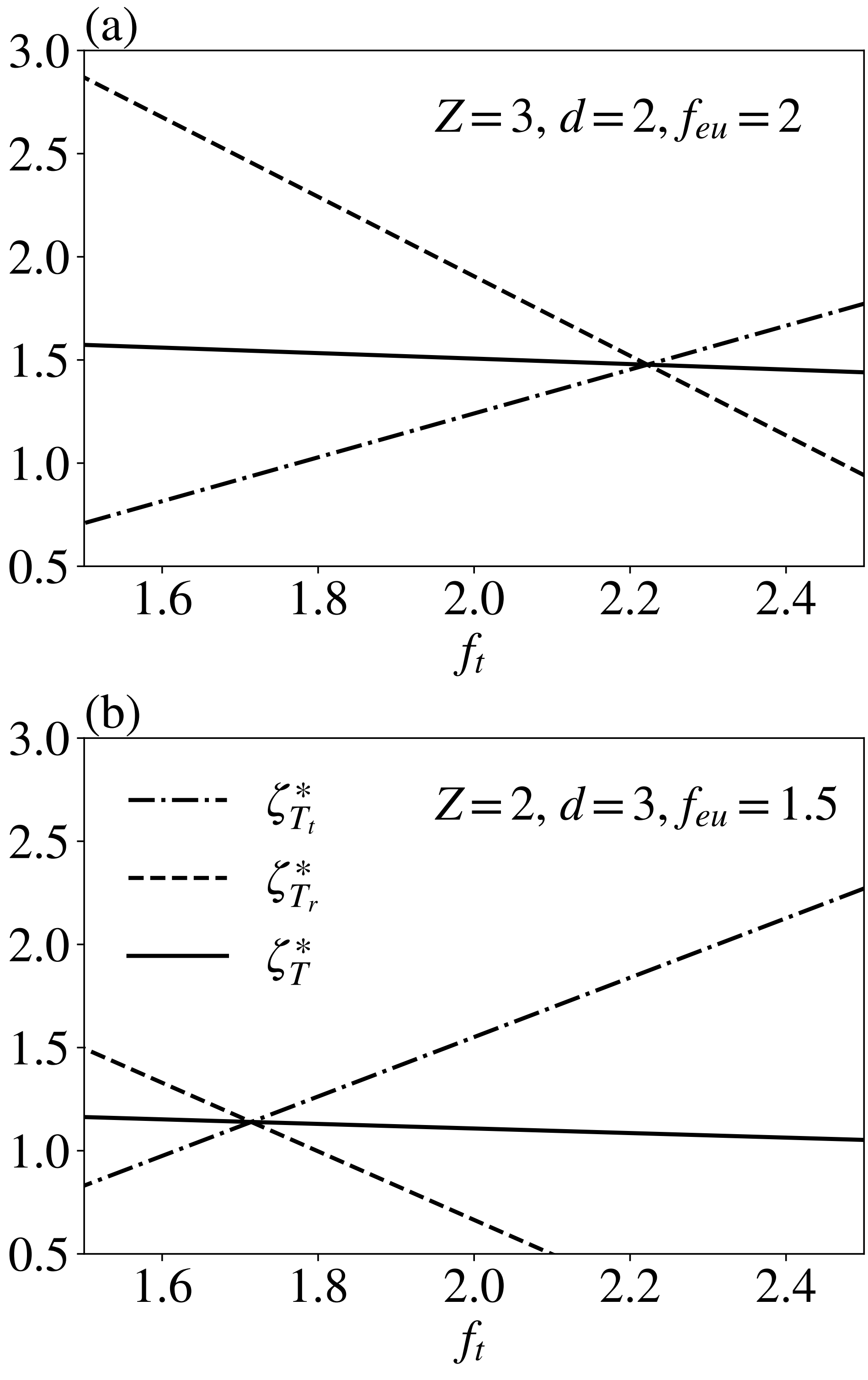
(a)
$Z = 3,\ d = 2,\ f_{eu} = 2$
3.0
2.5
2.0
1.5
1.0
0.5
1.6
1.8
2.0
2.2
2.4
f_t
(b)
$\zeta^*_{T_t}$
$\zeta^*_{T_r}$
ζ^*_{T}
$Z = 2,\ d = 3,\ f_{eu} = 1.5$
3.0
2.5
2.0
1.5
1.0
0.5
1.6
1.8
2.0
2.2
2.4
f_t

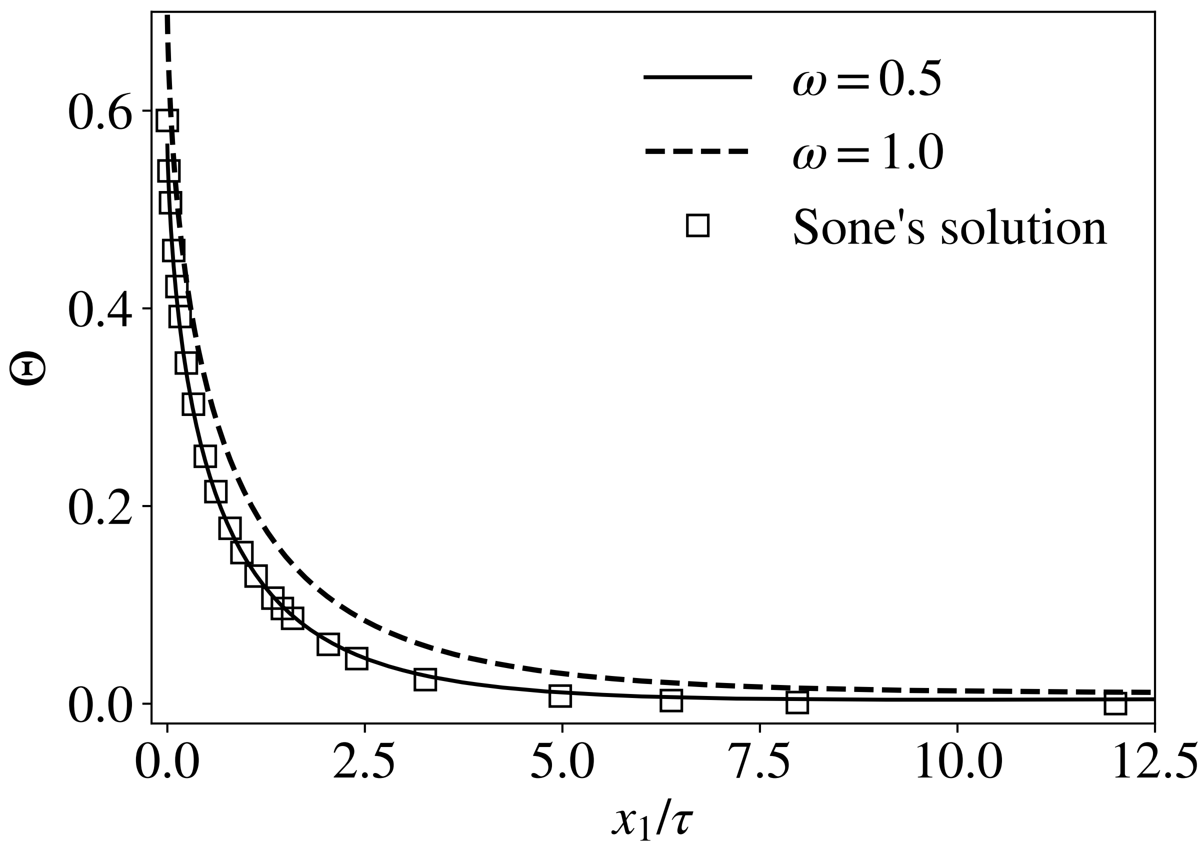
ω = 0.5
ω = 1.0
Sone's solution
Θ
0.0
0.2
0.4
0.6
0.0
2.5
5.0
7.5
10.0
12.5
x1/τ

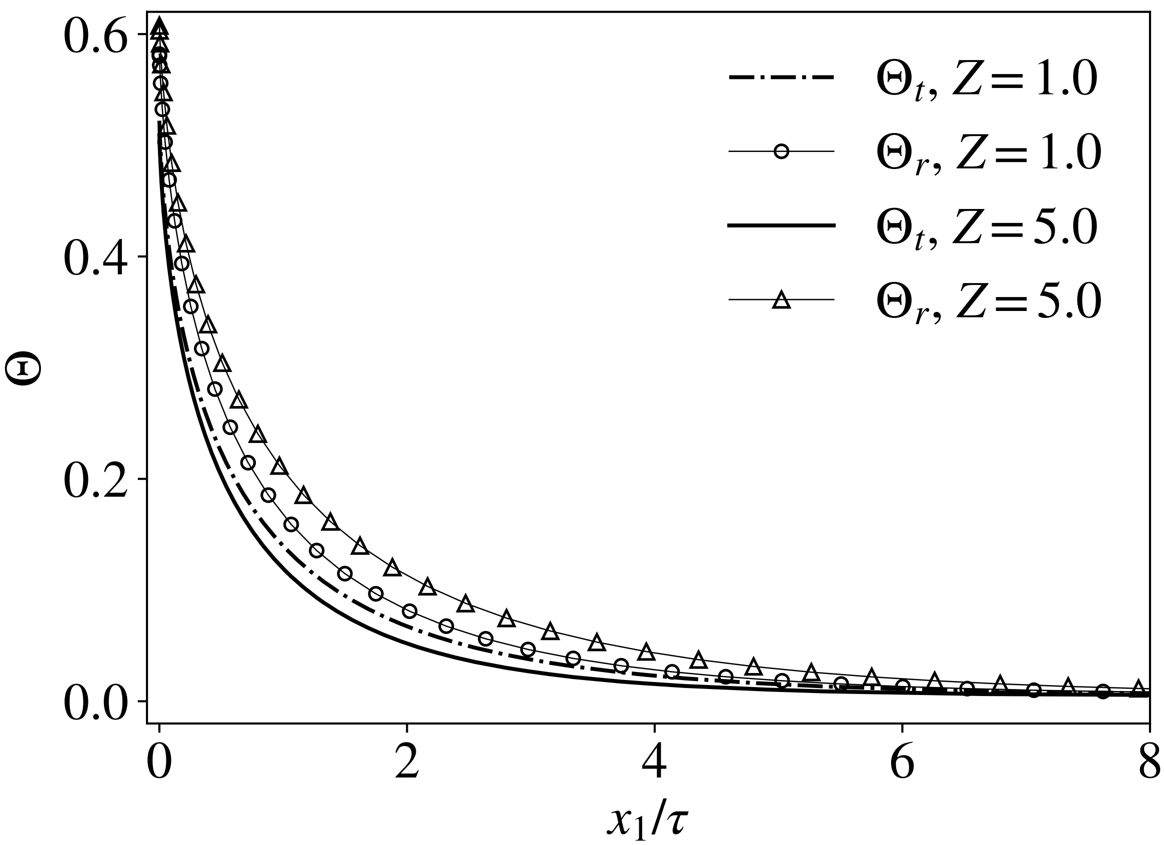
0.6
0.4
0.2
0.0
Θ
0
2
4
6
8
x_1/τ
Θ_t, $Z = 1.0$
Θ_r, $Z = 1.0$
Θ_t, $Z = 5.0$
Θ_r, $Z = 5.0$

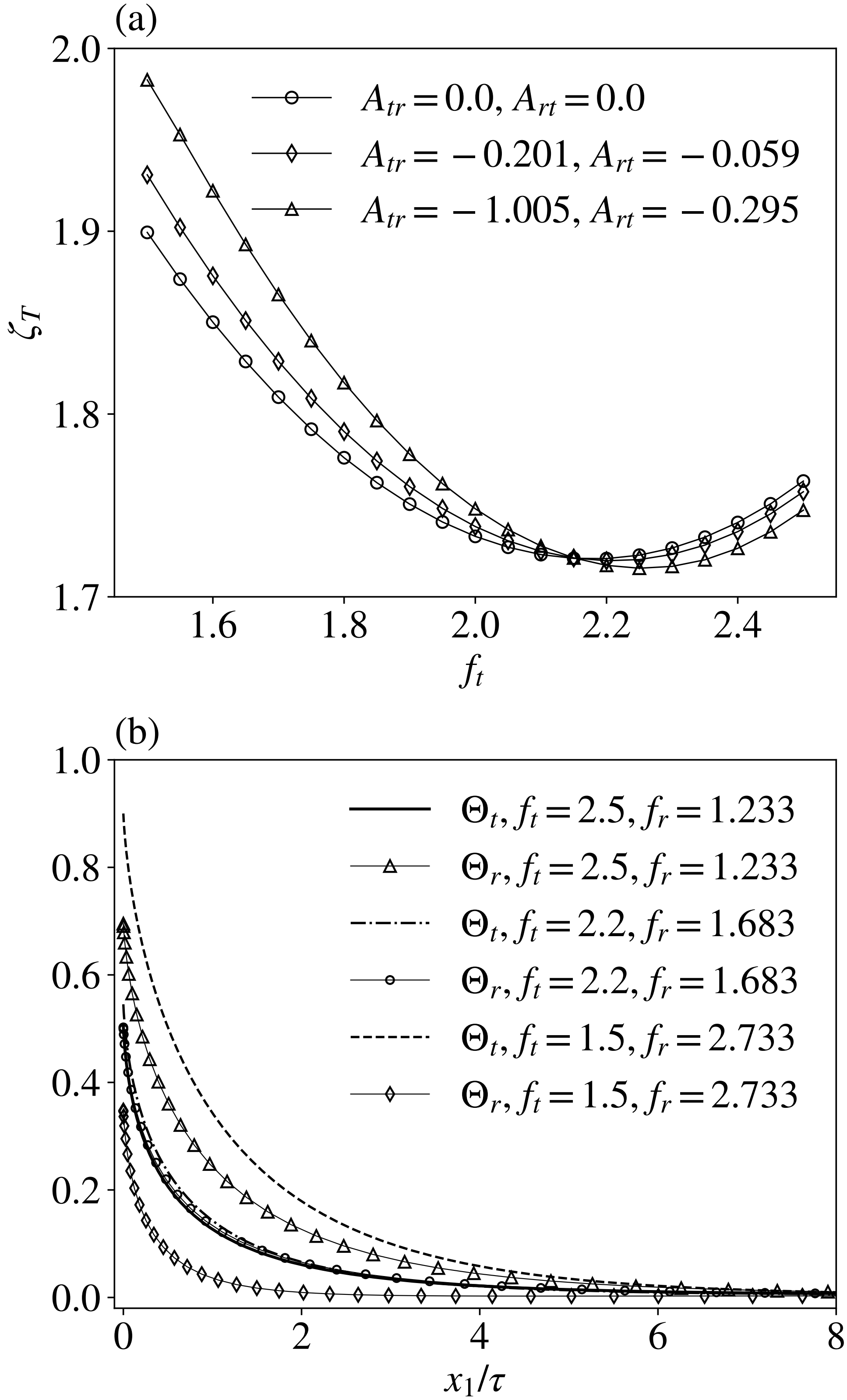
(a)
$A_{tr}=0.0, A_{rt}=0.0$
$A_{tr}=-0.201, A_{rt}=-0.059$
$A_{tr}=-1.005, A_{rt}=-0.295$
ζ_T
f_t
(b)
$\Theta_t, f_t=2.5, f_r=1.233$
$\Theta_r, f_t=2.5, f_r=1.233$
$\Theta_t, f_t=2.2, f_r=1.683$
$\Theta_r, f_t=2.2, f_r=1.683$
$\Theta_t, f_t=1.5, f_r=2.733$
$\Theta_r, f_t=1.5, f_r=2.733$
x_1/τ

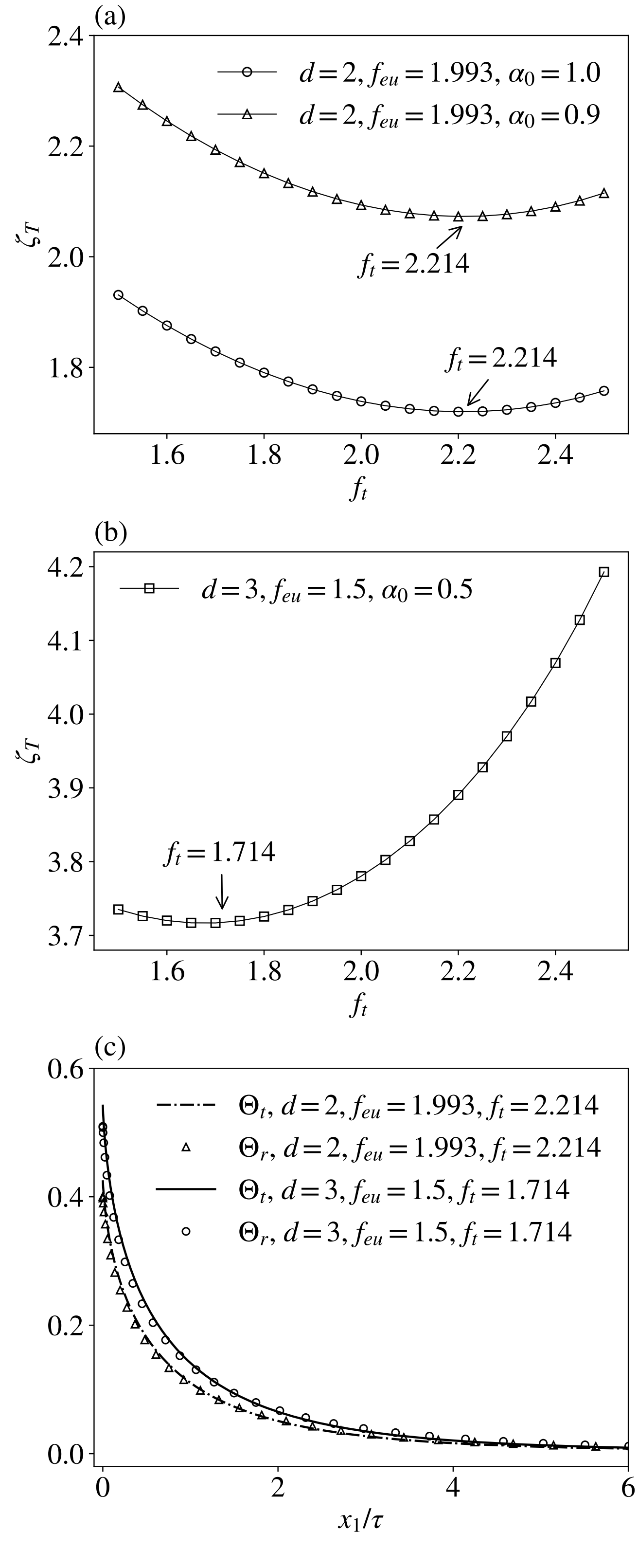
(a)
$d=2, f_{eu}=1.993, \alpha_0=1.0$
$d=2, f_{eu}=1.993, \alpha_0=0.9$
$f_t=2.214$
$f_t=2.214$
ζ_T
f_t
(b)
$d=3, f_{eu}=1.5, \alpha_0=0.5$
$f_t=1.714$
ζ_T
f_t
(c)
Θ_t, $d=2, f_{eu}=1.993, f_t=2.214$
Θ_r, $d=2, f_{eu}=1.993, f_t=2.214$
Θ_t, $d=3, f_{eu}=1.5, f_t=1.714$
Θ_r, $d=3, f_{eu}=1.5, f_t=1.714$
x_1/τ

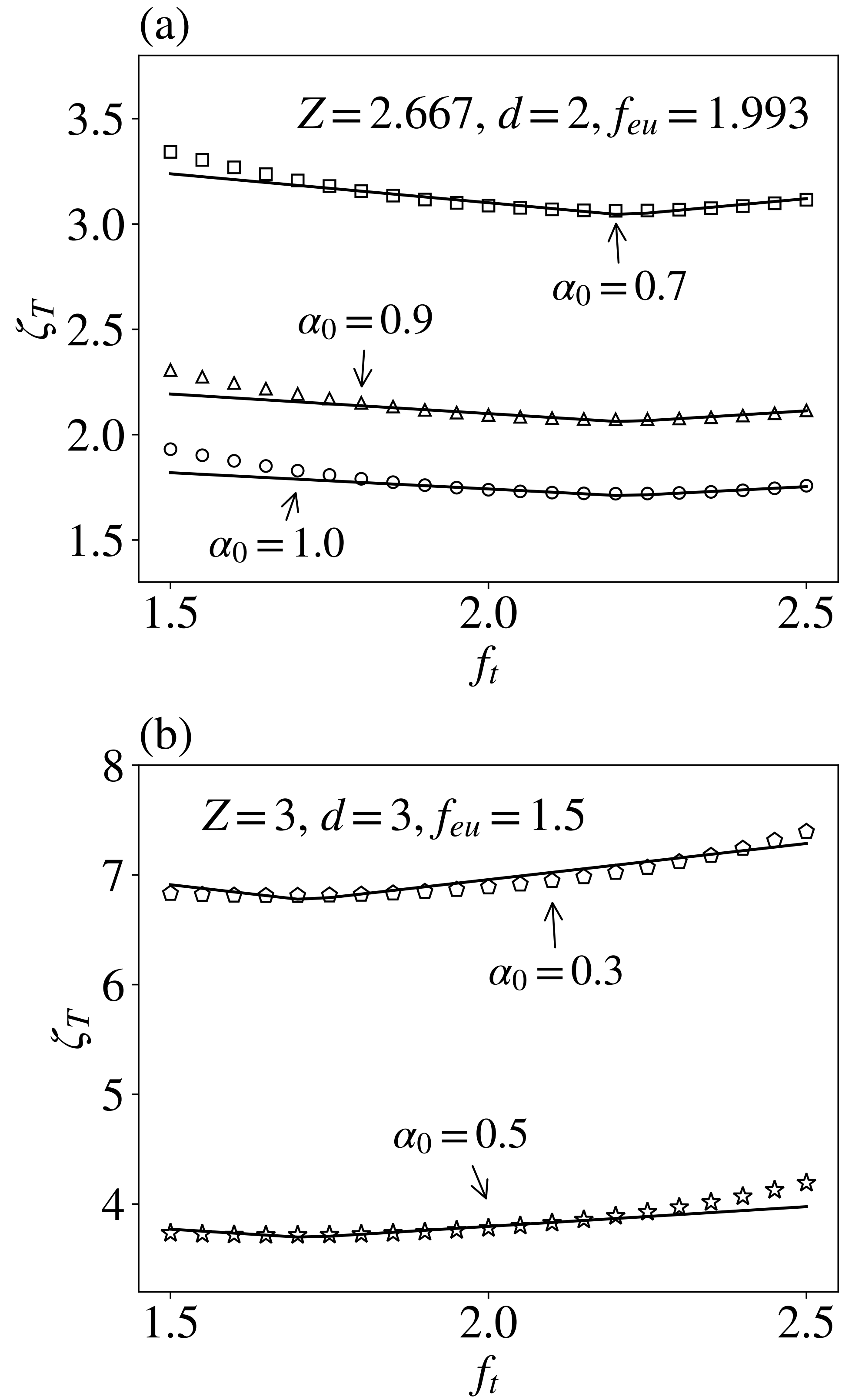
(a)
$Z=2.667,\ d=2,\ f_{eu}=1.993$
$\alpha_0=0.7$
$\alpha_0=0.9$
$\alpha_0=1.0$
ζ_T
f_t
(b)
$Z=3,\ d=3,\ f_{eu}=1.5$
$\alpha_0=0.3$
$\alpha_0=0.5$
ζ_T
f_t